ARTICLE IN PRESS

Available online at www.sciencedirect.com

ScienceDirect

Journal of Computational and Applied Mathematics ▮▮▮ (▮▮▮▮) ▮▮▮–▮▮▮

JOURNAL OF COMPUTATIONAL AND APPLIED MATHEMATICS

www.elsevier.com/locate/cam

Estimation of penalty parameters for symmetric interior penalty Galerkin methods

Yekaterina Epshteyn, Béatrice Rivière*, [1]

Department of Mathematics, University of Pittsburgh, 301 Thackeray, Pittsburgh, PA 15260, USA

Received 9 February 2006; received in revised form 9 August 2006

Abstract

This paper presents computable lower bounds of the penalty parameters for stable and convergent symmetric interior penalty Galerkin methods. In particular, we derive the explicit dependence of the coercivity constants with respect to the polynomial degree and the angles of the mesh elements. Numerical examples in all dimensions and for different polynomial degrees are presented. We show the numerical effects of loss of coercivity.

MSC: 65N30; 65N12

Keywords: Coercivity; Continuity; Stable versus unstable interior penalty method; Elliptic problems

1. Introduction

The symmetric interior penalty Galerkin (SIPG) method is an example of discontinuous Galerkin methods, which uses penalties to enforce weakly both continuity of the solution and the boundary conditions. For the elliptic problems, the bilinear form of the SIPG method was first introduced in [25] in a collocation finite element scheme. The SIPG method was extended to parabolic problems in [1,2]. A variation of the method was applied to biharmonic problems in [6]. Before its application to discontinuous finite element spaces, the inclusion of penalty terms in a variational formulation for the continuous finite element method can be found in several papers such as in [19,4,5,12].

Some of the general attractive features of the SIPG method are the local and high order of approximation, the flexibility due to local mesh refinement and the ability to handle unstructured meshes and discontinuous coefficients. More specific properties include the optimal error estimates in both the H^1 and L^2 norms and the resulting symmetric linear systems easily solved by standard solvers for symmetric matrices (such as conjugate gradient). The analysis and application of SIPG to a wide range of problems can be found in the literature: a non-exhaustive list is given in [7,8,10,14,20,22,23,17] and the references herein.

The SIPG method is obtained by integrating by parts on each mesh element, and summing over all elements. Two stabilization terms are then added: a symmetrizing term corresponding to fluxes obtained after integration by part, and a penalty term imposing a weak continuity of the numerical solution. It is well known that there exists a threshold penalty

* Corresponding author.
E-mail address: riviere@math.pitt.edu (B. Rivière).
[1] This research is partially funded by NSF-DMS 0506039.

0377-0427/$ - see front matter © 2006 Elsevier B.V. All rights reserved.
doi:10.1016/j.cam.2006.08.029

above which the bilinear form is coercive and the scheme is stable and convergent. Another related discontinuous Galerkin method is the non-symmetric interior penalty Galerkin (NIPG) method [21,15]: this method differs from the SIPG method by only one sign: the symmetrizing term is added instead of being subtracted. On one hand, the loss of symmetry in the scheme gives an immediate coercivity of the bilinear form: the NIPG scheme is stable and convergent for any value of the penalty. On the other hand, optimal error estimates in the L^2 norm cannot be proved via the standard Nitsche lift. As of today, this remains an open problem.

The objective of this work is to derive rigorous computable bounds of the threshold penalty that would yield a stable and convergent SIPG. We consider a general second order elliptic problem on a domain in any dimension, subdivided into simplices. Our main result is an improved coercivity result. In particular, we show that the constant of coercivity depends on quantities local to each mesh element, namely the local polynomial degree and the smallest $\sin\theta$ over all angles of the triangle in 2D or over all dihedral angles in the tetrahedron in 3D. We also investigate the effects of the penalty numerically and exhibit unstable oscillatory solutions for penalty values below the threshold penalty. Our results also apply to the incomplete interior penalty Galerkin method [11], that differs from SIPG and NIPG in the fact that the symmetrizing stabilizing term is removed. For this method, the error analysis in the energy norm is identical to the analysis of the SIPG method.

The outline of the paper is as follows: the model problem and scheme are presented in Section 2. Section 3 contains the improved coercivity and continuity theorems. Section 4 shows numerical examples in all dimensions that support our theoretical results. Some conclusions follow.

2. Model problem and scheme

Let Ω be a domain in $\mathbb{R}^d$, $d = 1, 2, 3$. Let the boundary of the domain $\partial\Omega$ be the union of two disjoint sets Γ_D and Γ_N. We denote $\mathbf{n}$ the unit normal vector to each edge of $\partial\Omega$ exterior of Ω. For f given in $L^2(\Omega)$, u_D given in $H^{1/2}(\Gamma_D)$ and u_N given in $L^2(\Gamma_N)$, we consider the following elliptic problem:

$$-\nabla\cdot(K\nabla u) + \alpha u = f \quad \text{in } \Omega, \tag{1}$$

$$u = u_D \quad \text{on } \Gamma_D, \tag{2}$$

$$K\nabla u\cdot\mathbf{n} = u_N \quad \text{on } \Gamma_N. \tag{3}$$

Here, the function α is a nonnegative scalar function and K is a matrix-valued function $K = (k_{ij})_{1\leqslant i,j\leqslant d}$ that is symmetric positive definite.

We can assume that the problem (1)–(3) has a unique solution in $H^1(\Omega)$ when $|\Gamma_D| > 0$ or when $\alpha \neq 0$. On the other hand, when $\partial\Omega = \Gamma_N$ and $\alpha = 0$, problem (1)–(3) has a solution in $H^1(\Omega)$ which is unique up to an additive constant, provided $\int_\Omega f = -\int_{\partial\Omega} g$.

Let $\mathcal{T}_h = \{E\}_E$ be a subdivision of Ω, where E is an interval if $d = 1$, a triangle if $d = 2$, or a tetrahedron if $d = 3$. Let

$$h = \max_{E\in\mathcal{T}_h} h_E,$$

where h_E is the diameter of E. We assume that for each element E, there exist two positive constants k_0^E and k_1^E such that

$$\forall\mathbf{x}\in E, \quad k_0^E\mathbf{x}^{\mathrm{T}}\mathbf{x} \leqslant \mathbf{x}^{\mathrm{T}}K\mathbf{x} \leqslant k_1^E\mathbf{x}^{\mathrm{T}}\mathbf{x}. \tag{4}$$

We also denote by k_0 (resp. k_1) the minimum (resp. maximum) of k_0^E (resp. k_1^E) over all elements E in $\mathcal{T}_h$.

To each element E, we associate a polynomial degree p^E, positive integer and we denote the vector $\mathbf{p} = \{p^E : E \in \mathcal{T}_h\}$. The finite element subspace is taken to be

$$\mathcal{D}_{\mathbf{p}}(\mathcal{T}_h) = \{v_h \in L^2(\Omega) : \forall E \in \mathcal{T}_h \quad v_h|_E \in \mathbb{P}_{p^E}(E)\},$$

where $\mathbb{P}_{p^E}(E)$ denotes the space of polynomials of total degree less than p^E on the element E. We note that there are no continuity constraints on the discontinuous finite element spaces. In what follows, we will denote by $\|\cdot\|_{\mathcal{O}}$ the L^2 norm over the domain $\mathcal{O}$.

Please cite this article as: Y. Epshteyn, B. Rivière, Estimation of penalty parameters for symmetric interior penalty Galerkin methods, Journal of Computational and Applied Mathematics (2006), doi: 10.1016/j.cam.2006.08.029

We now present the scheme. For readability purposes, we separate the 1D case from the higher dimensional case.

2.1. SIPG in one dimension

Assuming that $\Omega = (a, b)$, we can write the subdivision:

$$\mathscr{T}_h = \{I_{n+1} = (x_n, x_{n+1}) : n = 0, \ldots, N-1\}, \tag{5}$$

with $x_0 = a$ and $x_N = b$. We allow the mesh to be non-uniform. In this 1D setting, we simplify the notation and use $p^{(n)}$ for the polynomial degree on the interval I_n and the constants $k_0^{(n)}$, $k_1^{(n)}$ for the lower and upper bounds of K restricted to the interval I_n. For simplicity, we assume that $\Gamma_D = \{a, b\}$ and thus $\Gamma_N = \emptyset$.

If we denote $v(x_n^+) = \lim_{\varepsilon\to 0^+} v(x_n + \varepsilon)$ and $v(x_n^-) = \lim_{\varepsilon\to 0^+} v(x_n - \varepsilon)$, we can define the jump and average of v at the endpoints of I_n:

$$\forall n = 1, \ldots, N-1, \quad [v(x_n)] = v(x_n^-) - v(x_n^+), \quad \{v(x_n)\} = \tfrac{1}{2}(v(x_n^-) + v(x_n^+)),$$

$$[v(x_0)] = -v(x_0^+), \quad \{v(x_0)\} = v(x_0^+), \quad [v(x_N)] = v(x_N^-), \quad \{v(x_N)\} = v(x_N^-).$$

The SIPG finite element method for problem (1)–(3) is then: find u_h in $\mathscr{D}_{\mathbf{p}}(\mathscr{T}_h)$ such that

$$\forall v_h \in \mathscr{D}_{\mathbf{p}}(\mathscr{T}_h), \quad A(u_h, v_h) = L(v_h), \tag{6}$$

where the bilinear form A and linear form L are defined by

$$\begin{aligned} A(w, v) = {} & \sum_{n=0}^{N-1} \int_{x_n}^{x_{n+1}} (K(x)w'(x)v'(x) + \alpha w(x)v(x))\,\mathrm{d}x + \frac{\sigma_0}{|I_1|}[w(x_0)][v(x_0)] \\ & + \sum_{n=1}^{N-1} \left(\frac{\sigma_n^+}{2|I_{n+1}|} + \frac{\sigma_n^-}{2|I_n|}\right)[w(x_n)][v(x_n)] + \frac{\sigma_N}{|I_N|}[w(x_N)][v(x_N)] \\ & - \sum_{n=0}^{N} \{K(x_n)w'(x_n)\}[v(x_n)] - \sum_{n=0}^{N} \{K(x_n)v'(x_n)\}[w(x_n)], \end{aligned} \tag{7}$$

$$L(v) = \int_a^b f(x)v(x)\,\mathrm{d}x + K(a)v'(a)u_D(a) - K(b)v'(b)u_D(b) + \frac{\sigma_0}{|I_1|}\,v(a)u_D(a) + \frac{\sigma_N}{|I_N|}\,v(b)u_D(b), \tag{8}$$

where the penalty parameters σ_0, σ_N, $\{\sigma_n^+, \sigma_n^-\}_{1\leqslant n\leqslant N-1}$ are positive real numbers, all bounded below by $\sigma > 0$. The energy norm associated to A is

$$\begin{aligned} \forall\, v_h \in \mathscr{D}_{\mathbf{p}}(\mathscr{T}_h), \quad \|v_h\|_{\mathscr{E}} = {} & \left(\sum_{n=0}^{N-1} \int_{x_n}^{x_{n+1}} (K(x)^{1/2}(v_h'(x))^2 + \alpha(x)(v_h(x))^2)\,\mathrm{d}x \right. \\ & \left. + \frac{\sigma_0}{|I_1|}[v(x_0)]^2 + \sum_{n=1}^{N-1} \left(\frac{\sigma_n^+}{2|I_{n+1}|} + \frac{\sigma_n^-}{2|I_n|}\right)[v(x_n)]^2 + \frac{\sigma_N}{|I_N|}[v(x_N)]^2\right)^{1/2}. \end{aligned} \tag{9}$$

2.2. SIPG in high dimensions

Let Γ_h be the set of interior edges in 2D (or faces in 3D) of the subdivision $\mathscr{T}_h$. With each edge (or face) e, we associate a unit normal vector $\mathbf{n}_e$. If e is on the boundary $\partial\Omega$, then $\mathbf{n}_e$ is taken to be the unit outward vector to $\partial\Omega$.

We now define the average and the jump for w on an edge e shared by two elements E_e^1 and E_e^2:

$$\forall e = \partial E_e^1 \cap \partial E_e^2, \quad \{w\} = \tfrac{1}{2}(w|_{E_e^1}) + \tfrac{1}{2}(w|_{E_e^2}), \quad [w] = (w|_{E_e^1}) - (w|_{E_e^2}).$$

Please cite this article as: Y. Epshteyn, B. Rivière, Estimation of penalty parameters for symmetric interior penalty Galerkin methods, Journal of Computational and Applied Mathematics (2006), doi: 10.1016/j.cam.2006.08.029

For a boundary edge belonging to the boundary of E_e^1, we will use the same notation:

$$\forall e = \partial E_e^1 \cap \partial\Omega, \quad \{w\} = w|_{E_e^1}, \quad [w] = w|_{E_e^1}.$$

The general SIPG variational formulation of problem (1)–(3) is: find u_h in $\mathscr{D}_{\mathbf{p}}(\mathscr{T}_h)$ such that

$$\forall v_h \in \mathscr{D}_{\mathbf{p}}(\mathscr{T}_h), \quad A(u_h, v_h) = L(v_h), \tag{10}$$

where the bilinear form A and linear form L are defined by

$$A(w, v) = \sum_{E\in\mathscr{T}_h} \int_E K\nabla w \cdot \nabla v + \int_\Omega \alpha w v + \sum_{e\in\Gamma_h\cup\Gamma_D} \frac{\sigma_e}{|e|^{\beta_0}} \int_e [w][v]$$
$$- \sum_{e\in\Gamma_h\cup\Gamma_D} \int_e \{K\nabla w \cdot \mathbf{n}_e\}[v] - \sum_{e\in\Gamma_h\cup\Gamma_D} \int_e \{K\nabla v \cdot \mathbf{n}_e\}[w], \tag{11}$$

$$L(v) = \int_\Omega f v - \sum_{e\in\Gamma_D} \int_e (K\nabla v \cdot \mathbf{n}_e) u_D + \sum_{e\in\Gamma_D} \int_e \frac{\sigma_e}{|e|^{\beta_0}} v u_D + \sum_{e\in\Gamma_N} \int_e v u_N. \tag{12}$$

The penalty parameter σ_e is a positive constant on each edge (or face) e and we denote by $\sigma > 0$ the minimum of all σ_e. The parameter $\beta_0 > 0$ is a global constant that, in general, is chosen to be equal to $(d-1)^{-1}$. If $\beta_0 > (d-1)^{-1}$, then the SIPG method is said to be superpenalized. The energy norm associated to A is

$$\forall v_h \in \mathscr{D}_{\mathbf{p}}(\mathscr{T}_h), \quad \|v_h\|_{\mathscr{E}} = \left(\sum_{E\in\mathscr{T}_h} \int_E K(\nabla v_h)^2 + \int_\Omega \alpha v_h^2 + \sum_{e\in\Gamma_h\cup\Gamma_D} \frac{\sigma_e}{|e|^{\beta_0}} \int_e [v_h]^2 \right)^{1/2}. \tag{13}$$

2.3. Error analysis

We recall the well-known results about the schemes (6) and (10).

Lemma 1 (*Consistency*). *The exact solution of* (1)–(3) *satisfies the discrete variational problem* (6) *in one dimension and* (10) *in two or three dimensions*.

Lemma 2 (*Coercivity*). *Assume that for* $d = 2$ *or* 3, *the bound* $\beta_0 \geqslant (d-1)^{-1}$ *holds. Then, there exists a penalty* σ^* *that depends on* $\mathbf{p}$ *and* β_0 *such that if* $\sigma > \sigma^*$ *we have*

$$\forall v_h \in \mathscr{D}_{\mathbf{p}}(\mathscr{T}_h), \quad A(v_h, v_h) \geqslant C^* \|v_h\|_{\mathscr{E}}^2,$$

for some positive constant C^* *independent of* h.

Lemma 3 (*Continuity*). *Assume that for* $d = 2$ *or* 3, *the bound* $\beta_0 \geqslant (d-1)^{-1}$ *holds. Then, there exists a constant* $\tilde{C}$ *that depends on* $\mathbf{p}$ *and* β_0 *such that*

$$\forall v_h, w_h \in \mathscr{D}_{\mathbf{p}}(\mathscr{T}_h), \quad A(v_h, w_h) \leqslant \tilde{C} \|v_h\|_{\mathscr{E}} \|w_h\|_{\mathscr{E}}.$$

Theorem 4 (*Error estimates*). *Let* $\tilde{p} = \min\{p^E : E \in \mathscr{T}_h\}$ *and let* $u \in H^{\tilde{p}+1}(\Omega)$ *be the exact solution of* (1)–(3). *Assume that the coercivity lemma holds true. In addition, assume that* $\beta_0 = (d-1)^{-1}$. *Then, there is a constant* C *independent of* h, *but dependent of* $1/C^*$, *such that*

$$\|u - u_h\|_{\mathscr{E}} \leqslant C h^{\tilde{p}} |u|_{H^{\tilde{p}+1}(\Omega)}.$$

The condition on β_0 *can be relaxed to* $\beta_0 \geqslant (d-1)^{-1}$ *if either* $|\Gamma_D| = 0$ *or* $|\Gamma_D| > 0$ *and* u_D *can be extended by zero to a function in* $\mathscr{D}_{\mathbf{p}}(\mathscr{T}_h)$.

These results are proved by using standard trace inequalities [9] and they can be found for example in [2,3,16].

Please cite this article as: Y. Epshteyn, B. Rivière, Estimation of penalty parameters for symmetric interior penalty Galerkin methods, Journal of Computational and Applied Mathematics (2006), doi: 10.1016/j.cam.2006.08.029

The aim of this work is to determine exactly the value σ^* that would guarantee the coercivity and thus the convergence of the method. We also obtain a precise expression for both coercivity and continuity constants C^*, $\tilde{C}$. We then show numerically that for penalty values lower than σ^*, unstable solutions could occur.

3. Improved coercivity and continuity lemmas

We will consider each dimension separately as the details of the proofs differ.

3.1. Estimation of σ^* in one dimension

We recall that N is the number of intervals in the subdivision (5).

Theorem 5. *For any vector of positive numbers $\boldsymbol{\epsilon} = (\varepsilon^{(n)})_{n=1}^N$, define*

$$\sigma_0^* = \frac{2}{\varepsilon^{(1)}} \frac{(k_1^{(1)})^2}{k_0^{(1)}} (p^{(1)})^2, \tag{14}$$

$$\sigma_N^* = \frac{2}{\varepsilon^{(N)}} \frac{(k_1^{(N)})^2}{k_0^{(N)}} (p^{(N)})^2, \tag{15}$$

$$\forall n = 1, \dots N-1, \quad \sigma_n^{*-} = \frac{1}{\varepsilon^{(n)}} \frac{(k_1^{(n)})^2}{k_0^{(n)}} (p^{(n)})^2, \tag{16}$$

$$\forall n = 1, \dots N-1, \quad \sigma_n^{*+} = \frac{1}{\varepsilon^{(n+1)}} \frac{(k_1^{(n+1)})^2}{k_0^{(n+1)}} (p^{(n+1)})^2. \tag{17}$$

Then, if for all n, $0 < \varepsilon^{(n)} < 1$, $\sigma_n^- > \sigma_n^{*-}$, $\sigma_n^+ > \sigma_n^{*+}$ and $\sigma_0 > \sigma_0^*$, $\sigma_N > \sigma_N^*$, there is a constant $0 < C^*(\boldsymbol{\epsilon}) < 1$, independent of h, such that

$$\forall v_h \in \mathscr{D}_{\mathbf{p}}(\mathscr{T}_h), \quad A(v_h, v_h) \geqslant C^*(\boldsymbol{\epsilon}) \|v_h\|_{\mathscr{E}}^2.$$

Moreover, an expression for $C^*(\boldsymbol{\epsilon})$ is

$$C^*(\boldsymbol{\epsilon}) = \min \left\{ \min_{n=1,\dots,N} (1 - \varepsilon^{(n)}), 1 - \frac{\sigma_0^*}{\sigma_0}, 1 - \frac{\sigma_N^*}{\sigma_N}, \min_{n=1,\dots,N-1} \left(1 - \frac{\sigma_n^{*-}}{\sigma_n^-}\right), \min_{n=1,\dots,N-1} \left(1 - \frac{\sigma_n^{*+}}{\sigma_n^+}\right) \right\}.$$

Proof. Choosing $w = v$ in (7) yields

$$A(v, v) = \sum_{n=0}^{N-1} \int_{x_n}^{x_{n+1}} (K(x) v'(x)^2 + \alpha(x) v(x)^2) \, \mathrm{d}x - 2 \sum_{n=0}^{N} \{K(x_n) v'(x_n)\} [v(x_n)]$$
$$+ \frac{\sigma_0}{|I_1|} [v(x_0)]^2 + \sum_{n=1}^{N-1} \left(\frac{\sigma_n^+}{2|I_{n+1}|} + \frac{\sigma_n^-}{2|I_n|} \right) [v(x_n)]^2 + \frac{\sigma_N}{|I_N|} [v(x_N)]^2. \tag{18}$$

It suffices to bound the term $-2 \sum_{n=0}^{N} \{K(x_n) v'(x_n)\} [v(x_n)]$ and obtain some restrictions on the penalty parameters for the coercivity to hold. Let us first consider the interior points. By definition of the average and the property (4), we have for $1 \leqslant n \leqslant N-1$:

$$|\{K(x_n) v'(x_n)\}| \leqslant \frac{k_1^{(n)}}{2} |v'(x_n^-)| + \frac{k_1^{(n+1)}}{2} |v'(x_n^+)|. \tag{19}$$

Please cite this article as: Y. Epshteyn, B. Rivière, Estimation of penalty parameters for symmetric interior penalty Galerkin methods, Journal of Computational and Applied Mathematics (2006), doi: 10.1016/j.cam.2006.08.029

For any interval $I = (s, t)$, the following improved inverse trace inequality holds [24]:

$$\forall v_h \in \mathbb{P}_p(I), \quad |v_h(s)| \leqslant \frac{p+1}{\sqrt{|I|}} \|v_h\|_I. \tag{20}$$

Hence using (20) we can bound $|v'(x_n^-)|$ and $|v'(x_n^+)|$:

$$|v'(x_n^-)| \leqslant \frac{p^{(n)}}{\sqrt{|I_n|}} \|v'\|_{I_n}, \quad |v'(x_n^+)| \leqslant \frac{p^{(n+1)}}{\sqrt{|I_{n+1}|}} \|v'\|_{I_{n+1}}.$$

Using these bounds we obtained for the interior point x_n of the subdivision:

$$\begin{aligned}\{K(x_n)v'(x_n)\}[v(x_n)] &\leqslant \|v'\|_{I_n} \frac{k_1^{(n)} p^{(n)}}{2\sqrt{|I_n|}} |[v(x_n)]| + \|v'\|_{I_{n+1}} \frac{k_1^{(n+1)} p^{(n+1)}}{2\sqrt{|I_{n+1}|}} |[v(x_n)]| \\ &\leqslant \sqrt{\varepsilon^{(n)}} \|K^{1/2} v'\|_{I_n} \frac{k_1^{(n)} p^{(n)}}{2\sqrt{k_0^{(n)}}\sqrt{\varepsilon^{(n)}}} \frac{|[v(x_n)]|}{\sqrt{|I_n|}} \\ &\quad + \sqrt{\varepsilon^{(n+1)}} \|K^{1/2} v'\|_{I_{n+1}} \frac{k_1^{(n+1)} p^{(n+1)}}{2\sqrt{k_0^{(n+1)}}\sqrt{\varepsilon^{(n+1)}}} \frac{|[v(x_n)]|}{\sqrt{|I_{n+1}|}}.\end{aligned} \tag{21}$$

Let us consider now the boundary nodes x_0 and x_N:

$$\begin{aligned}\{K(x_0)v'(x_0)\}[v(x_0)] &\leqslant |K(x_0)v'(x_0)[v(x_0)]| \\ &\leqslant \sqrt{\varepsilon^{(1)}} \|K^{1/2} v'\|_{I_1} \frac{k_1^{(1)} p^{(1)}}{\sqrt{k_0^{(1)}}\sqrt{\varepsilon^{(1)}}} \frac{|[v(x_0)]|}{\sqrt{|I_1|}},\end{aligned} \tag{22}$$

$$\begin{aligned}\{K(x_N)v'(x_N)\}[v(x_N)] &\leqslant |K(x_N)v'(x_N)[v(x_N)]| \\ &\leqslant \sqrt{\varepsilon^{(N)}} \|K^{1/2} v'\|_{I_N} \frac{k_1^{(N)} p^{(N)}}{\sqrt{k_0^{(N)}}\sqrt{\varepsilon^{(N)}}} \frac{|[v(x_N)]|}{\sqrt{|I_N|}}.\end{aligned} \tag{23}$$

Combining the bounds above gives

$$\begin{aligned}\sum_{n=0}^{N} \{K(x_n)v'(x_n)\}[v(x_n)] &\leqslant \sqrt{\varepsilon^{(1)}} \|K^{1/2} v'\|_{I_1} \frac{k_1^{(1)} p^{(1)}}{\sqrt{k_0^{(1)}}\sqrt{\varepsilon^{(1)}}} \frac{|[v(x_0)]|}{\sqrt{|I_1|}} \\ &\quad + \sum_{n=1}^{N-1} \left(\sqrt{\varepsilon^{(n)}} \|K^{1/2} v'\|_{I_n} \frac{k_1^{(n)} p^{(n)}}{2\sqrt{k_0^{(n)}}\sqrt{\varepsilon^{(n)}}} \frac{|[v(x_n)]|}{\sqrt{|I_n|}} \right. \\ &\quad \left. + \sqrt{\varepsilon^{(n+1)}} \|K^{1/2} v'\|_{I_{n+1}} \frac{k_1^{(n+1)} p^{(n+1)}}{2\sqrt{k_0^{(n+1)}}\sqrt{\varepsilon^{(n+1)}}} \frac{|[v(x_n)]|}{\sqrt{|I_{n+1}|}} \right) \\ &\quad + \sqrt{\varepsilon^{(N)}} \|K^{1/2} v'\|_{I_N} \frac{k_1^{(N)} p^{(N)}}{\sqrt{k_0^{(N)}}\sqrt{\varepsilon^{(N)}}} \frac{|[v(x_N)]|}{\sqrt{|I_N|}}.\end{aligned}$$

Please cite this article as: Y. Epshteyn, B. Rivière, Estimation of penalty parameters for symmetric interior penalty Galerkin methods, Journal of Computational and Applied Mathematics (2006), doi: 10.1016/j.cam.2006.08.029

After application of Cauchy–Shwarz's inequality we have

$$\sum_{n=0}^{N}\{K(x_n)v'(x_n)\}[v(x_n)] \leqslant \left(\varepsilon^{(1)}\|K^{1/2}v'\|_{I_1}^2 + \sum_{n=1}^{N-1}(\varepsilon^{(n)}\|K^{1/2}v'\|_{I_n}^2 + \varepsilon^{(n+1)}\|K^{1/2}v'\|_{I_{n+1}}^2) + \varepsilon^{(N)}\|K^{1/2}v'\|_{I_N}^2\right)^{1/2}$$
$$\left(\frac{(k_1^{(1)}p^{(1)})^2}{k_0^{(1)}\varepsilon^{(1)}}\frac{|[v(x_0)]|^2}{|I_1|} + \sum_{n=1}^{N-1}\left(\frac{(k_1^{(n)}p^{(n)})^2}{2k_0^{(n)}\varepsilon^{(n)}}\frac{|[v(x_n)]|^2}{2|I_n|} + \frac{(k_1^{(n+1)}p^{(n+1)})^2}{2k_0^{(n+1)}\varepsilon^{(n+1)}}\frac{|[v(x_n)]|^2}{2|I_{n+1}|}\right) + \frac{(k_1^{(N)}p^{(N)})^2}{k_0^{(N)}\varepsilon^{(N)}}\frac{|[v(x_N)]|^2}{|I_N|}\right)^{1/2}$$
$$\leqslant \left(\sum_{n=1}^{N}\varepsilon^{(n)}\|K^{1/2}v'\|_{I_n}^2\right)^{1/2}\left(\frac{2(k_1^{(1)}p^{(1)})^2}{k_0^{(1)}\varepsilon^{(1)}}\frac{|[v(x_0)]|^2}{|I_1|} + \sum_{n=1}^{N-1}\left(\frac{(k_1^{(n)}p^{(n)})^2}{k_0^{(n)}\varepsilon^{(n)}}\frac{|[v(x_n)]|^2}{2|I_n|} + \frac{(k_1^{(n+1)}p^{(n+1)})^2}{k_0^{(n+1)}\varepsilon^{(n+1)}}\frac{|[v(x_n)]|^2}{2|I_{n+1}|}\right) + \frac{2(k_1^{(N)}p^{(N)})^2}{k_0^{(N)}\varepsilon^{(N)}}\frac{|[v(x_N)]|^2}{|I_N|}\right)^{1/2}.$$

Application of Young's inequality yields

$$\sum_{n=0}^{N}\{K(x_n)v'(x_n)\}[v(x_n)] \leqslant \sum_{n=1}^{N}\frac{\varepsilon^{(n)}}{2}\|K^{1/2}v'\|_{I_n}^2 + \frac{(k_1^{(1)}p^{(1)})^2}{k_0^{(1)}\varepsilon^{(1)}}\frac{|[v(x_0)]|^2}{|I_1|}$$
$$+ \sum_{n=1}^{N-1}\left(\frac{(k_1^{(n)}p^{(n)})^2}{2k_0^{(n)}\varepsilon^{(n)}}\frac{|[v(x_n)]|^2}{2|I_n|} + \frac{(k_1^{(n+1)}p^{(n+1)})^2}{2k_0^{(n+1)}\varepsilon^{(n+1)}}\frac{|[v(x_n)]|^2}{2|I_{n+1}|}\right)$$
$$+ \frac{(k_1^{(N)}p^{(N)})^2}{k_0^{(N)}\varepsilon^{(N)}}\frac{|[v(x_N)]|^2}{|I_N|}.$$

Hence using the inequality above, we obtain a lower bound for the right-hand side of (18)

$$A(v,v) \geqslant \sum_{n=1}^{N}(1-\varepsilon^{(n)})\|K^{1/2}v'\|_{I_n}^2 + \sum_{n=1}^{N}\|\alpha^{1/2}v\|_{I_n}^2 + \left(\sigma_0 - 2\frac{(k_1^{(1)}p^{(1)})^2}{k_0^{(1)}\varepsilon^{(1)}}\right)\frac{|[v(x_0)]|^2}{|I_1|}$$
$$+ \sum_{n=1}^{N-1}\left(\left(\sigma_n^- - \frac{(k_1^{(n)}p^{(n)})^2}{k_0^{(n)}\varepsilon^{(n)}}\right)\frac{|[v(x_n)]|^2}{2|I_n|} + \left(\sigma_n^+ - \frac{(k_1^{(n+1)}p^{(n+1)})^2}{k_0^{(n+1)}\varepsilon^{(n+1)}}\right)\frac{|[v(x_n)]|^2}{2|I_{n+1}|}\right)$$
$$+ \left(\sigma_N - 2\frac{(k_1^{(N)}p^{(N)})^2}{k_0^{(N)}\varepsilon^{(N)}}\right)\frac{|[v(x_N)]|^2}{|I_N|}. \tag{24}$$

From (24) the bilinear form (7) is coercive if

$$\varepsilon^{(n)} < 1 \quad \forall n = 1,\ldots,N, \tag{25}$$

Please cite this article as: Y. Epshteyn, B. Rivière, Estimation of penalty parameters for symmetric interior penalty Galerkin methods, Journal of Computational and Applied Mathematics (2006), doi: 10.1016/j.cam.2006.08.029

and

$$\begin{cases} \sigma_0 > \dfrac{2(k_1^{(1)} p^{(1)})^2}{k_0^{(1)} \varepsilon^{(1)}} \\ \sigma_N > \dfrac{2(k_1^{(N)} p^{(N)})^2}{k_0^{(N)} \varepsilon^{(N)}} \\ \sigma_n^- > \dfrac{(k_1^{(n)} p^{(n)})^2}{k_0^{(n)} \varepsilon^{(n)}} \qquad \forall\, n = 1, \ldots, N-1, \\ \sigma_n^+ > \dfrac{(k_1^{(n+1)} p^{(n+1)})^2}{k_0^{(n+1)} \varepsilon^{(n+1)}} \qquad \forall\, n = 1, \ldots, N-1. \end{cases} \tag{26}$$

This concludes the proof. □

Similarly, one can show the following improved continuity constant.

Lemma 6. *Under the notation of Theorem* 5, *the continuity constant* $\tilde{C}$ *of Lemma* 3 *is given by*

$$\tilde{C} = \max \left\{ \max_{n=1,\ldots,N} (1 + \varepsilon^{(n)}), 1 + \frac{\sigma_0^*}{\sigma_0}, 1 + \frac{\sigma_N^*}{\sigma_N}, \max_{n=1,\ldots,N-1} \left(1 + \frac{\sigma_n^{*-}}{\sigma_n^-}, 1 + \frac{\sigma_n^{*+}}{\sigma_n^+} \right) \right\}.$$

Corollary 7. *The threshold value for the penalty parameter is obtained by taking* $\varepsilon^{(n)} = 1$ *in* (26)

$$\begin{cases} \sigma_0^{**} = \dfrac{2(k_1^{(1)} p^{(1)})^2}{k_0^{(1)}} \\ \sigma_N^{**} = \dfrac{2(k_1^{(N)} p^{(N)})^2}{k_0^{(N)}} \\ \sigma_n^{**-} = \dfrac{(k_1^{(n)} p^{(n)})^2}{k_0^{(n)}} \qquad \forall\, n = 1, \ldots, N-1, \\ \sigma_n^{**+} = \dfrac{(k_1^{(n+1)} p^{(n+1)})^2}{k_0^{(n+1)}} \qquad \forall\, n = 1, \ldots, N-1. \end{cases} \tag{27}$$

Remark 8. A straightforward consequence is an estimate of the threshold value in the case where the same polynomial degree p is used everywhere:

$$\begin{cases} \sigma_n^{**} = 2 \dfrac{k_1^2}{k_0} p^2, \qquad n = 0, N, \\ \sigma_n^{**-} = \sigma_n^{**+} = \dfrac{k_1^2}{k_0} p^2 \qquad \forall\, n = 1, \ldots, N-1, \end{cases} \tag{28}$$

where we recall that k_0 and k_1 are the global lower and upper bounds of K.

3.2. Estimation of σ^* in two dimensions

In this section, we denote θ_E the smallest angle in a triangle E. This corresponds to the smallest $\sin\theta$ over all angles θ of E. We show that the penalty parameters depend on θ_E, p^E and the bounds k_0^E, k_1^E.

Please cite this article as: Y. Epshteyn, B. Rivière, Estimation of penalty parameters for symmetric interior penalty Galerkin methods, Journal of Computational and Applied Mathematics (2006), doi: 10.1016/j.cam.2006.08.029

Theorem 9. *Let $\varepsilon = (\varepsilon^E)_{E\in\mathcal{T}_h}$ be a vector of positive components such that ε^E is associated to the triangle E in $\mathcal{T}_h$. Assume that $\beta_0 = 1$. For any edge $e \in \Gamma_h$ shared by E_e^1 and E_e^2, define*

$$\sigma_e^* = \frac{3(k_1^{E_e^1})^2}{2k_0^{E_e^1}\varepsilon^{E_e^1}}(p^{E_e^1})(p^{E_e^1}+1)\cot\theta_{E_e^1} + \frac{3(k_1^{E_e^2})^2}{2k_0^{E_e^2}\varepsilon^{E_e^2}}(p^{E_e^2})(p^{E_e^2}+1)\cot\theta_{E_e^2}. \tag{29}$$

For any boundary edge $e \in \Gamma_D \cap \partial E_e^1$, define

$$\sigma_e^* = \frac{6(k_1^{E_e^1})^2}{k_0^{E_e^1}\varepsilon^{E_e^1}}(p^{E_e^1})(p^{E_e^1}+1)\cot\theta_{E_e^1}. \tag{30}$$

Then if $\sigma_e > \sigma_e^*$ for all $e \in \Gamma_h \cup \Gamma_D$, there is a constant $0 < C^*(\varepsilon) < 1$, independent of h, such that

$$\forall v_h \in \mathcal{D}_{\mathbf{p}}(\mathcal{T}_h), \quad A(v_h, v_h) \geqslant C^*(\varepsilon)\|v_h\|_{\mathscr{E}}^2.$$

An expression for C^* is

$$C^*(\varepsilon) = \min\left\{\min_{E\in\mathcal{T}_h}(1-\varepsilon^E), \min_{e\in\Gamma_h\cup\Gamma_D}\left(1-\frac{\sigma_e^*}{\sigma_e}\right)\right\}.$$

Proof. Similarly, as in the 1D case, we choose $w = v$ in (11):

$$A(v,v) = \sum_{E\in\mathcal{T}_h}\int_E K\nabla v\cdot\nabla v + \int_\Omega \alpha v^2 - 2\sum_{e\in\Gamma_h\cup\Gamma_D}\int_e \{K\nabla v\cdot\mathbf{n}_e\}[v] + \sum_{e\in\Gamma_h\cup\Gamma_D}\frac{\sigma_e}{|e|}\int_e [v]^2. \tag{31}$$

In order to have coercivity of the bilinear form we need to bound the term $-2\sum_{e\in\Gamma_h\cup\Gamma_D}\int_e\{K\nabla v\cdot\mathbf{n}_e\}[v]$.

Let us first consider one interior edge e shared by two triangles E_e^1 and E_e^2. Applying Cauchy–Schwarz inequality we have

$$\int_e \{K\nabla v\cdot\mathbf{n}_e\}[v] \leqslant \|\{K\nabla v\cdot\mathbf{n}_e\}\|_e\|[v]\|_e. \tag{32}$$

Using the definition of the average and the property (4), we have

$$\|\{K\nabla v\cdot\mathbf{n}_e\}\|_e \leqslant \frac{k_1^{E_e^1}}{2}\|\nabla v|_{E_e^1}\|_e + \frac{k_1^{E_e^2}}{2}\|\nabla v|_{E_e^2}\|_e, \tag{33}$$

so we obtain for the interior edge e:

$$\int_e \{K\nabla v\cdot\mathbf{n}_e\}[v] \leqslant \left(\frac{k_1^{E_e^1}}{2}\|\nabla v|_{E_e^1}\|_e + \frac{k_1^{E_e^2}}{2}\|\nabla v|_{E_e^2}\|_e\right)\|[v]\|_e. \tag{34}$$

Similarly, for a boundary edge e belonging to the boundary of element E_e^1:

$$\int_e \{K\nabla v\cdot\mathbf{n}_e\}[v] \leqslant k_1^{E_e^1}\|\nabla v|_{E_e^1}\|_e\|[v]\|_e. \tag{35}$$

We now recall the inverse inequality valid on an edge of a triangle E [24]:

$$\forall v_h \in \mathbb{P}_{p^E}(E), \quad \|v_h\|_e \leqslant \sqrt{\frac{(p^E+1)(p^E+2)}{2}\frac{|e|}{|E|}}\|v_h\|_E. \tag{36}$$

Hence in (36) we need to estimate the ratio $|e|/|E|$, where e is one edge of a triangle E. For this, we consider a triangle with edges e_1, e_2 and e_3. We denote by θ_{ij} the interior angle between edge e_i and edge e_j (see Fig. 1). Without loss of generality, we assume that $e = e_3$.

Please cite this article as: Y. Epshteyn, B. Rivière, Estimation of penalty parameters for symmetric interior penalty Galerkin methods, Journal of Computational and Applied Mathematics (2006), doi: 10.1016/j.cam.2006.08.029

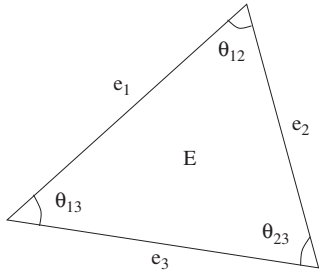

Fig. 1. Angles and edges in a generic triangle.

The area of the triangle E is given by the formula:

$$|E| = \tfrac{1}{2}\,|e_i||e_j|\sin\theta_{ij} = \tfrac{1}{4}\,|e_3||e_1|\sin\theta_{13} + \tfrac{1}{4}\,|e_3||e_2|\sin\theta_{23}.$$

The length of the edge e in the triangle E can also be written as

$$|e| = |e_3| = |e_1|\cos\theta_{13} + |e_2|\cos\theta_{23}.$$

Hence, using the smallest angle θ_E in the triangle E we have

$$\frac{|e|}{|E|} = \frac{4}{|e|}\left(\frac{|e_1|\cos\theta_{13} + |e_2|\cos\theta_{23}}{|e_1|\sin\theta_{13} + |e_2|\sin\theta_{23}}\right) \leqslant \frac{4}{|e|}\left(\frac{|e_1|\cos\theta_E + |e_2|\cos\theta_E}{|e_1|\sin\theta_E + |e_2|\sin\theta_E}\right).$$

So we obtain the following estimate:

$$\frac{|e|}{|E|} \leqslant \frac{4\cot\theta_E}{|e|}. \tag{37}$$

Then using inverse inequality (36), and the estimate (37) in (34) we obtain for the interior edge e shared by the triangles E_e^1 and E_e^2

$$\begin{aligned}\int_e \{K\nabla v\cdot\mathbf{n_e}\}[v] \leqslant{}& \sqrt{\varepsilon^{E_e^1}}\,\|K^{1/2}\nabla v\|_{E_e^1}\,\frac{k_1^{E_e^1}}{\sqrt{k_0^{E_e^1}}\sqrt{\varepsilon^{E_e^1}}}\sqrt{\frac{p^{E_e^1}(p^{E_e^1}+1)\cot\theta_{E_e^1}}{2}}\,\frac{\|[v]\|_e}{\sqrt{|e|}}\\ &+\sqrt{\varepsilon^{E_e^2}}\,\|K^{1/2}\nabla v\|_{E_e^2}\,\frac{k_1^{E_e^2}}{\sqrt{k_0^{E_e^2}}\sqrt{\varepsilon^{E_e^2}}}\sqrt{\frac{p^{E_e^2}(p^{E_e^2}+1)\cot\theta_{E_e^2}}{2}}\,\frac{\|[v]\|_e}{\sqrt{|e|}}.\end{aligned} \tag{38}$$

Repeating the argument for a boundary edge that belongs to ∂E_e^1, we obtain

$$\int_e \{K\nabla v\cdot\mathbf{n}_e\}[v] \leqslant \sqrt{\varepsilon^{E_e^1}}\,\|K^{1/2}\nabla v\|_{E_e^1}\,\frac{k_1^{E_e^1}}{\sqrt{k_0^{E_e^1}}\sqrt{\varepsilon^{E_e^1}}}\sqrt{2p^{E_e^1}(p^{E_e^1}+1)\cot\theta_{E_e^1}}\,\frac{\|[v]\|_e}{\sqrt{|e|}}. \tag{39}$$

Please cite this article as: Y. Epshteyn, B. Rivière, Estimation of penalty parameters for symmetric interior penalty Galerkin methods, Journal of Computational and Applied Mathematics (2006), doi: 10.1016/j.cam.2006.08.029

Combining the bounds above and using Cauchy–Schwarz's inequality, we obtain

$$\sum_{e\in\Gamma_h\cup\Gamma_D}\int_e\{K\nabla v\cdot\mathbf{n}_e\}[v]\leqslant\left(3\sum_{E\in\mathscr{E}_h}\varepsilon^E\left\|K^{1/2}\nabla v\right\|_E^2\right)^{1/2}$$
$$\times\left(\sum_{e\in\Gamma_h}\left(\frac{(k_1^{E_e^1})^2p^{E_e^1}(p^{E_e^1}+1)\cot\theta_{E_e^1}}{2k_0^{E_e^1}\varepsilon^{E_e^1}}\frac{\|[v]\|_e^2}{|e|}+\frac{(k_1^{E_e^2})^2p^{E_e^2}(p^{E_e^2}+1)\cot\theta_{E_e^2}}{2k_0^{E_e^2}\varepsilon^{E_e^2}}\frac{\|[v]\|_e^2}{|e|}\right)\right.$$
$$\left.+\sum_{e\in\Gamma_D}\frac{2(k_1^{E_e^1})^2p^{E_e^1}(p^{E_e^1}+1)\cot\theta_{E_e^1}}{k_0^{E_e^1}\varepsilon^{E_e^1}}\frac{\|[v]\|^2}{|e|}\right)^{1/2}. \tag{40}$$

Therefore, by using Young's inequality, we have

$$\sum_{e\in\Gamma_h\cup\Gamma_D}\int_e\{K\nabla v\cdot\mathbf{n}_e\}[v]\leqslant\sum_{E\in\mathscr{E}_h}\frac{\varepsilon^E}{2}\|K^{1/2}\nabla v\|_e^2+\sum_{e\in\Gamma_h}\left(\frac{3(k_1^{E_e^1})^2p^{E_e^1}(p^{E_e^1}+1)\cot\theta_{E_e^1}}{4k_0^{E_e^1}\varepsilon^{E_e^1}}\frac{\|[v]\|_e^2}{|e|}\right.$$
$$\left.+\frac{3(k_1^{E_e^2})^2p^{E_e^2}(p^{E_e^2}+1)\cot\theta_{E_e^2}}{4k_0^{E_e^2}\varepsilon^{E_e^2}}\frac{\|[v]\|_e^2}{|e|}\right)+\sum_{e\in\Gamma_D}\frac{3(k_1^{E_e^1})^2p^{E_e^1}(p^{E_e^1}+1)\cot\theta_{E_e^1}}{k_0^{E_e^1}\varepsilon^{E_e^1}}\frac{\|[v]\|^2}{|e|}. \tag{41}$$

Therefore, using the estimate (41) we have the following lower bound for the right-hand side of (31):

$$A(v,v)\geqslant\sum_{E\in\mathscr{T}_h}(1-\varepsilon^E)\|K^{1/2}\nabla v\|_E^2+\sum_{E\in\mathscr{T}_h}\|\alpha^{1/2}v\|_E^2$$
$$+\sum_{e\in\Gamma_h}\left(\sigma_e-\frac{3}{2k_0^{E_e^1}\varepsilon^{E_e^1}}(k_1^{E_e^1})^2(p^{E_e^1})(p^{E_e^1}+1)\cot\theta_{E_e^1}\right.$$
$$\left.-\frac{3}{2k_0^{E_e^2}\varepsilon^{E_e^2}}(k_1^{(E_e^2)})^2(p^{E_e^2})(p^{E_e^2}+1)\cot\theta_{E_e^2}\right)\frac{\|[v]\|_e^2}{|e|}$$
$$+\sum_{e\in\Gamma_D}\left(\sigma_e-\frac{6}{k_0^{E_e^1}\varepsilon^{E_e^1}}(k_1^{E_e^1})^2(p^{E_e^1})(p^{E_e^1}+1)\cot\theta_{E_e^1}\right)\frac{\|[v]\|_e^2}{|e|}. \tag{42}$$

From (42) the bilinear form (11) is coercive if the following conditions hold:

$$\forall E\in\mathscr{T}_h,\quad\varepsilon^E<1, \tag{43}$$

$$\forall e\in\Gamma_h,\quad\sigma_e>\frac{3(k_1^{E_e^1})^2}{2k_0^{E_e^1}\varepsilon^{E_e^1}}(p^{E_e^1})(p^{E_e^1}+1)\cot\theta_{E_e^1}+\frac{3(k_1^{(E_e^2)})^2}{2k_0^{E_e^2}\varepsilon^{E_e^2}}(p^{E_e^2})(p^{E_e^2}+1)\cot\theta_{E_e^2}, \tag{44}$$

$$\forall e\in\Gamma_D,\quad\sigma_e>\frac{6(k_1^{E_e^1})^2}{k_0^{E_e^1}\varepsilon^{E_e^1}}(p^{E_e^1})(p^{E_e^1}+1)\cot\theta_{E_e^1}. \tag{45}$$

This concludes the proof. □

Please cite this article as: Y. Epshteyn, B. Rivière, Estimation of penalty parameters for symmetric interior penalty Galerkin methods, Journal of Computational and Applied Mathematics (2006), doi: 10.1016/j.cam.2006.08.029

Lemma 10. *Under the notation of Theorem* 9, *the continuity constant* $\tilde{C}$ *of Lemma* 3 *is given by*

$$\tilde{C} = \max\left\{ \max_{E\in\mathscr{T}_h}(1+\varepsilon^E), \max_{e\in\Gamma_h\cup\Gamma_D}\left(1+\frac{\sigma_e^*}{\sigma_e}\right)\right\}.$$

Corollary 11. *The threshold value for the penalty parameter is obtained by taking* $\varepsilon^E = 1$ *in* (44) *and* (45)

$$\forall e\in\Gamma_h,\quad \sigma_e^{**} = \frac{3(k_1^{E_e^1})^2}{2k_0^{E_e^1}}(p^{E_e^1})(p^{E_e^1}+1)\cot\theta_{E_e^1} + \frac{3(k_1^{(E_e^2)})^2}{2k_0^{E_e^2}}(p^{E_e^2})(p^{E_e^2}+1)\cot\theta_{E_e^2}, \tag{46}$$

$$\forall e\in\Gamma_D,\quad \sigma_e^{**} = \frac{6(k_1^{E_e^1})^2}{k_0^{E_e^1}}(p^{E_e^1})(p^{E_e^1}+1)\cot\theta_{E_e^1}. \tag{47}$$

Remark 12. Let $\theta_{\mathscr{T}}$ denote the smallest angle over all triangles in the subdivision. Assume that the same polynomial degree p is used everywhere. An estimate of the threshold value is then:

$$\forall e\in\Gamma_h,\quad \sigma_e^{**} = \frac{3k_1^2}{k_0}p(p+1)\cot\theta_{\mathscr{T}}, \tag{48}$$

$$\forall e\in\Gamma_D,\quad \sigma_e^{**} = \frac{6k_1^2}{k_0}p(p+1)\cot\theta_{\mathscr{T}}. \tag{49}$$

Remark 13. Similar results can be obtained in the case where superpenalization is used, namely $\beta_0 > 1$. The new values for the penalty parameters σ_e^*, σ_e^{**} are simply the ones obtained for the case $\beta_0 = 1$, times the quantity $|e|^{\beta_0-1}$.

3.3. Estimation of σ^* *in three dimensions*

In this section, we denote θ_E the dihedral angle in the tetrahedron E such that $\sin\theta_E$ is the smallest value for $\sin\theta$ over all dihedral angles θ of E. As in the 2D case, we show that the coercivity constant depends on θ_E. In Section 4, we outline an algorithm for computing such angle.

Theorem 14. *Let* $\varepsilon = (\varepsilon^E)_{E\in\mathscr{T}_h}$ *be a vector of positive components such that* ε^E *is associated to the tetrahedron* E *in* $\mathscr{T}_h$. *Assume that* $\beta_0 = 1/2$. *For any face* $e\in\Gamma_h$ *shared by* E_e^1 *and* E_e^2, *define*

$$\sigma_e^* = \frac{3}{2}\frac{(k_1^{E_e^1})^2}{k_0^{E_e^1}\varepsilon^{E_e^1}}p^{E_e^1}(p^{E_e^1}+2)(\cot\theta_{E_e^1})h|e|^{-1/2} + \frac{3}{2}\frac{(k_1^{E_e^2})^2}{k_0^{E_e^2}\varepsilon^{E_e^2}}p^{E_e^2}(p^{E_e^2}+2)(\cot\theta_{E_e^2})h|e|^{-1/2}.$$

For any boundary face $e\in\Gamma_D\cap\partial E_e^1$, *define*

$$\sigma_e^* = 6\frac{(k_1^{E_e^1})^2}{k_0^{E_e^1}\varepsilon^{E_e^1}}p^{(E_e^1)}(p^{E_e^1}+2)(\cot\theta_{E_e^1})h|e|^{-1/2}. \tag{50}$$

Then if $\sigma_e > \sigma_e^*$ *for all* $e\in\Gamma_h\cup\Gamma_D$, *there is a constant* $0 < C^*(\varepsilon) < 1$, *independent of* h, *such that*

$$\forall v_h\in\mathscr{D}_{\mathbf{p}}(\mathscr{T}_h),\quad A(v_h,v_h)\geqslant C^*(\varepsilon)\|v_h\|_{\mathscr{E}}^2.$$

Please cite this article as: Y. Epshteyn, B. Rivière, Estimation of penalty parameters for symmetric interior penalty Galerkin methods, Journal of Computational and Applied Mathematics (2006), doi: 10.1016/j.cam.2006.08.029

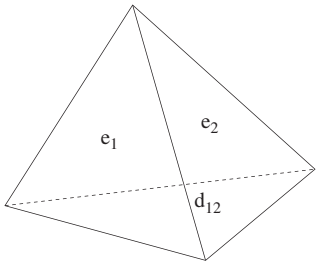

Fig. 2. A tetrahedral element with faces e_i.

An expression for C^* is

$$C^*(\varepsilon) = \min\left\{ \min_{E\in\mathscr{T}_h}(1-\varepsilon^E), \min_{e\in\Gamma_h\cup\Gamma_D}\left(1-\frac{\sigma_e^*}{\sigma_e}\right)\right\}.$$

Proof. The proof is similar to the one for the 2D case, and thus we will skip some technical details. We first recall the inverse inequality in 3D for a tetrahedral element E with face e [24]:

$$\forall v_h \in \mathbb{P}_{p^E}(E), \quad \|v_h\|_e \leqslant \sqrt{\frac{(p^E+1)(p^E+3)}{3}\frac{|e|}{|E|}}\,\|v_h\|_E. \tag{51}$$

Here, $|e|$ is the area of the face and $|E|$ is the volume of the tetrahedral element. So as in the case of the triangle we need to estimate the ratio $|e|/|E|$. For this, we fix an element E in $\mathscr{T}_h$ and we denote by e_i, $i=1,\ldots,4$ the faces of E and by d_{ij} the common edge to faces e_i and e_j. We will assume that the face e is denoted by e_4. We also denote by θ_{ij} the dihedral angle between faces e_i and e_j. A schematic is given in Fig. 2. The volume of the tetrahedron is given by the formula [18]:

$$|E| = \frac{2}{3|d_{ij}|}|e_i||e_j|\sin\theta_{ij}, \tag{52}$$

therefore, we can rewrite the volume as

$$\begin{aligned}|E| &= \frac{1}{3}\left(\frac{2}{3|d_{14}|}|e_4||e_1|\sin\theta_{14} + \frac{2}{3|d_{24}|}|e_4||e_2|\sin\theta_{24} + \frac{2}{3|d_{34}|}|e_4||e_3|\sin\theta_{34}\right)\\ &= \frac{2}{9}|e_4|\left(\frac{|e_1|}{d_{14}}\sin\theta_{14} + \frac{|e_2|}{d_{24}}\sin\theta_{24} + \frac{|e_3|}{d_{34}}\sin\theta_{34}\right).\end{aligned} \tag{53}$$

Hence, using the fact that $|d_{ij}|\leqslant h$, we have

$$\begin{aligned}\frac{|e|}{|E|} = \frac{|e_4|}{|E|} &= \frac{|e_4|}{(2/9)|e_4|((|e_1|/|d_{14}|)\sin\theta_{14} + (|e_2|/|d_{24}|)\sin\theta_{24} + (|e_3|/|d_{34}|)\sin\theta_{34})}\\ &\leqslant \frac{9}{2|e_4|}\frac{|e_4|}{((|e_1|/h)\sin\theta_{14} + (|e_2|/h)\sin\theta_{24} + (|e_3|/h)\sin\theta_{34})}\\ &\leqslant \frac{9}{2}\frac{h}{|e_4|}\frac{|e_4|}{(|e_1|\sin\theta_{14} + |e_2|\sin\theta_{24} + |e_3|\sin\theta_{34})}.\end{aligned} \tag{54}$$

Please cite this article as: Y. Epshteyn, B. Rivière, Estimation of penalty parameters for symmetric interior penalty Galerkin methods, Journal of Computational and Applied Mathematics (2006), doi: 10.1016/j.cam.2006.08.029

The relation between areas of the faces and dihedral angles in a general tetrahedron is given by the formula [18]:

$$|e_k| = \sum_{\substack{i=1 \\ i\neq k}}^{4} |e_i| \cos\theta_{ki}. \tag{55}$$

Hence we have using (55) in (54) and using dihedral angle θ_E defined above

$$\begin{aligned}\frac{|e|}{|E|} &\leqslant \frac{9}{2}\frac{h}{|e_4|}\left(\frac{|e_1|\cos\theta_{14}+|e_2|\cos\theta_{24}+|e_3|\cos\theta_{34}}{|e_1|\sin\theta_{14}+|e_2|\sin\theta_{24}+|e_3|\sin\theta_{34}}\right)\\ &\leqslant \frac{9}{2}\frac{h}{|e_4|}\left(\frac{|e_1||\cos\theta_E|+|e_2||\cos\theta_E|+|e_3||\cos\theta_E|}{|e_1|\sin\theta_E+|e_2|\sin\theta_E+|e_3|\sin\theta_E}\right).\end{aligned}$$

Therefore, we obtain the following estimate for a given face e in tetrahedral element E:

$$\frac{|e|}{|E|} \leqslant \frac{9}{2}\frac{h|\cot\theta_E|}{|e|}, \tag{56}$$

which is similar to estimate (37). Using a similar argument as in the triangular case, we obtain for the interior face e shared by the tetrahedral elements E_e^1 and E_e^2:

$$\begin{aligned}\int_e \{K\nabla v\cdot\mathbf{n}_e\}[v] \leqslant{}& \sqrt{\varepsilon^{E_e^1}}\|K^{1/2}\nabla v\|_{E_e^1}\frac{k_1^{E_e^1}}{\sqrt{k_0^{E_e^1}}\sqrt{\varepsilon^{E_e^1}}}\sqrt{\frac{3}{8}\,p^{E_e^1}(p^{E_e^1}+2)\cot\theta_{E_e^1}h}\,\frac{\|[v]\|_e}{\sqrt{|e|}}\\ &+\sqrt{\varepsilon^{E_e^2}}\|K^{1/2}\nabla v\|_{E_e^2}\frac{k_1^{E_e^2}}{\sqrt{k_0^{E_e^2}}\sqrt{\varepsilon^{E_e^2}}}\sqrt{\frac{3}{8}\,p^{E_e^2}(p^{E_e^2}+2)\cot\theta_{E_e^2}h}\,\frac{\|[v]\|_e}{\sqrt{|e|}}.\end{aligned} \tag{57}$$

and for a boundary face belonging to ∂E_e^1, we have

$$\int_e \{K\nabla v\cdot\mathbf{n}_e\}[v] \leqslant \sqrt{\varepsilon^{E_e^1}}\|K^{1/2}\nabla v\|_{E_e^1}\frac{k_1^{E_e^1}}{\sqrt{k_0^{E_e^1}}\sqrt{\varepsilon^{E_e^1}}}\sqrt{\frac{3}{2}\,p^{E_e^1}(p^{E_e^1}+2)\cot\theta_{E_e^1}h}\,\frac{\|[v]\|_e}{\sqrt{|e|}}. \tag{58}$$

Therefore, we can estimate now the term $\sum_{e\in\Gamma_h\cup\Gamma_D}\int_e\{K\nabla v\cdot\mathbf{n}_e\}[v]$. We first apply Cauchy–Schwarz's inequality. It is easy to see that we obtain

$$\begin{aligned}\sum_{e\in\Gamma_h\cup\Gamma_D}\int_e\{K\nabla v\cdot\mathbf{n}_e\}[v] \leqslant{}& \sum_{E\in\mathscr{T}_h}\frac{\varepsilon^E}{2}\|K^{1/2}\nabla v\|_E^2+\sum_{e\in\Gamma_h}\left(\frac{3}{4}\frac{(k_1^{E_e^1})^2}{k_0^{E_e^1}\varepsilon^{E_e^1}}p^{E_e^1}(p^{E_e^1}+2)\cot\theta_{E_e^1}h|e|^{-1/2}\right.\\ &\left.+\frac{3}{4}\frac{(k_1^{E_e^2})^2}{k_0^{E_e^2}\varepsilon^{E_e^2}}\,p^{E_e^2}(p^{E_e^2}+2)\cot\theta_{E_e^2}h|e|^{-1/2}\right)\frac{\|[v]\|_e^2}{|e|^{1/2}}\\ &+\sum_{e\in\Gamma_D}\left(3\,\frac{(k_1^{E_e^1})^2}{k_0^{E_e^1}\varepsilon^{E_e^1}}\,p^{E_e^1}(p^{E_e^1}+2)\cot\theta_{E_e^1}h|e|^{-1/2}\right)\frac{\|[v]\|_e^2}{|e|^{1/2}}.\end{aligned} \tag{59}$$

Please cite this article as: Y. Epshteyn, B. Rivière, Estimation of penalty parameters for symmetric interior penalty Galerkin methods, Journal of Computational and Applied Mathematics (2006), doi: 10.1016/j.cam.2006.08.029

Therefore, using the estimate (59) we have the following bound for the right-hand side of (31):

$$A(v,v) \geqslant \sum_{E\in\mathscr{E}_h}(1-\varepsilon^E)\|K^{1/2}\nabla v\|_E^2 + \sum_{E\in\mathscr{E}_h}\|\alpha^{1/2}v\|_E^2$$
$$+\sum_{e\in\Gamma_h}\left(\sigma_e - \frac{3}{2}\frac{(k_1^{E_e^1})^2}{k_0^{E_e^1}\varepsilon^{E_e^1}}\,p^{E_e^1}(p^{E_e^1}+2)\cot\theta_{E_e^1}h|e|^{-1/2}\right.$$
$$\left.-\frac{3}{2}\frac{(k_1^{E_e^2})^2}{k_0^{E_e^2}\varepsilon^{E_e^2}}\,p^{E_e^2}(p^{E_e^2}+2)\cot\theta_{E_e^2}h|e|^{-1/2}\right)\frac{\|[v]\|_e^2}{|e|^{1/2}}$$
$$+\sum_{e\in\Gamma_D}\left(\sigma_e - 6\frac{(k_1^{E_e^1})^2}{k_0^{E_e^1}\varepsilon^{E_e^1}}\,p^{E_e^1}(p^{E_e^1}+2)\cot\theta_{E_e^1}h|e|^{-1/2}\right)\frac{\|[v]\|_e^2}{|e|^{1/2}}. \tag{60}$$

Coercivity is then obtained for ε and σ_e satisfying the bounds:

$$\forall E\in\mathscr{T}_h,\quad \varepsilon^E<1, \tag{61}$$

$$\forall e\in\Gamma_h,\quad \sigma_e > \frac{3}{2}\frac{(k_1^{E_e^1})^2}{k_0^{E_e^1}\varepsilon^{E_e^1}}\,p^{E_e^1}(p^{E_e^1}+2)\cot\theta_{E_e^1}h|e|^{-1/2} + \frac{3}{2}\frac{(k_1^{E_e^2})^2}{k_0^{E_e^2}\varepsilon^{E_e^2}}\,p^{E_e^2}(p^{E_e^2}+2)\cot\theta_{E_e^2}h|e|^{-1/2}, \tag{62}$$

$$\forall e\in\Gamma_D,\quad \sigma_e > 6\frac{(k_1^{E_e^1})^2}{k_0^{E_e^1}\varepsilon^{E_e^1}}\,p^{E_e^1}(p^{E_e^1}+2)\cot\theta_{E_e^1}h|e|^{-1/2}. \tag{63}$$

This concludes the proof. □

Lemma 15. *Under the notation of Theorem* 14, *the continuity constant* $\tilde{C}$ *of Lemma* 3 *is given by*

$$\tilde{C} = \max\left\{\max_{E\in\mathscr{T}_h}(1+\varepsilon^E),\ \max_{e\in\Gamma_h\cup\Gamma_D}\left(1+\frac{\sigma_e^*}{\sigma_e}\right)\right\}.$$

Corollary 16. *The threshold value for the penalty parameter is obtained by taking* $\varepsilon^E=1$ *in* (62) *and* (63).

$$\forall e\in\Gamma_h,\quad \sigma_e^{**} = \frac{3}{2}\frac{(k_1^{E_e^1})^2}{k_0^{E_e^1}}\,p^{E_e^1}(p^{E_e^1}+2)\cot\theta_{E_e^1}h|e|^{-1/2} + \frac{3}{2}\frac{(k_1^{E_e^2})^2}{k_0^{E_e^2}}\,p^{E_e^2}(p^{E_e^2}+2)\cot\theta_{E_e^2}h|e|^{-1/2}, \tag{64}$$

$$\forall e\in\Gamma_D,\quad \sigma_e^{**} = 6\frac{(k_1^{E_e^1})^2}{k_0^{E_e^1}}\,p^{E_e^1}(p^{E_e^1}+2)\cot\theta_{E_e^1}h|e|^{-1/2}. \tag{65}$$

Remark 17. Let $\theta_{\mathscr{T}}$ denote the dihedral angle such that it gives the smallest $\sin\theta$ over all dihedral angles θ in the subdivision. Assume that the same polynomial degree p is used everywhere. An estimate of the threshold value is then:

$$\forall e\in\Gamma_h,\quad \sigma_e^{**} = \frac{3k_1^2}{k_0}\,p(p+2)h|e|^{-1/2}\cot\theta_{\mathscr{T}}, \tag{66}$$

$$\forall e\in\Gamma_D,\quad \sigma_e^{**} = \frac{6k_1^2}{k_0}\,p(p+2)h|e|^{-1/2}\cot\theta_{\mathscr{T}}. \tag{67}$$

Remark 18. As in the 2D case, if superpenalization is used, namely $\beta_0>1/2$, it is easy to show that the new values for the penalty parameters σ_e^*, σ_e^{**} are simply the ones obtained for the case $\beta_0=1/2$, times the quantity $|e|^{\beta_0-1/2}$.

Please cite this article as: Y. Epshteyn, B. Rivière, Estimation of penalty parameters for symmetric interior penalty Galerkin methods, Journal of Computational and Applied Mathematics (2006), doi: 10.1016/j.cam.2006.08.029

4. Numerical examples

We now present simple computations obtained for the domains Ω_1, Ω_2, Ω_3 in 1D, 2D and 3D, respectively. The exact solutions are periodic functions defined by

$$u_1(x) = \cos(8\pi x) \quad \text{on } \Omega_1 = (0, 1),$$

$$u_2(x) = \cos(8\pi x) + \cos(8\pi y) \quad \text{on } \Omega_2 = (0, 1)^2,$$

$$u_3(x) = \cos(8\pi x) + \cos(8\pi y) + \cos(8\pi z) \quad \text{on } \Omega_3 = (0, 1)^3.$$

The tensor K is the identity tensor. We vary the number of elements $\mathcal{N}_h$ in the mesh, the polynomial degree and the penalty value (denoted by σ) that is chosen constant over the whole domain, unless specified otherwise. In each case, we compute the limiting penalty value σ^{**} given by (28) in 1D, (48)–(49) in 2D and (66)–(67) in 3D.

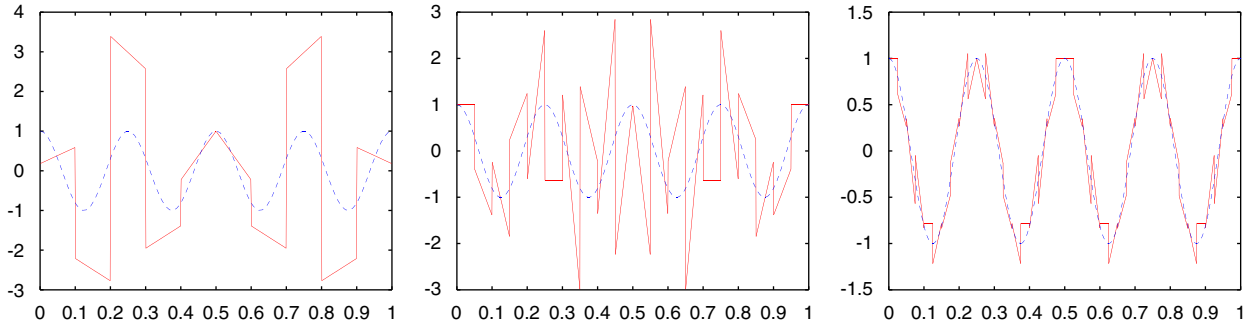

Fig. 3. $p = 1$, $\sigma = 0.5$: $\mathcal{N}_h = 10$ (left), $\mathcal{N}_h = 20$ (center), $\mathcal{N}_h = 40$ (right).

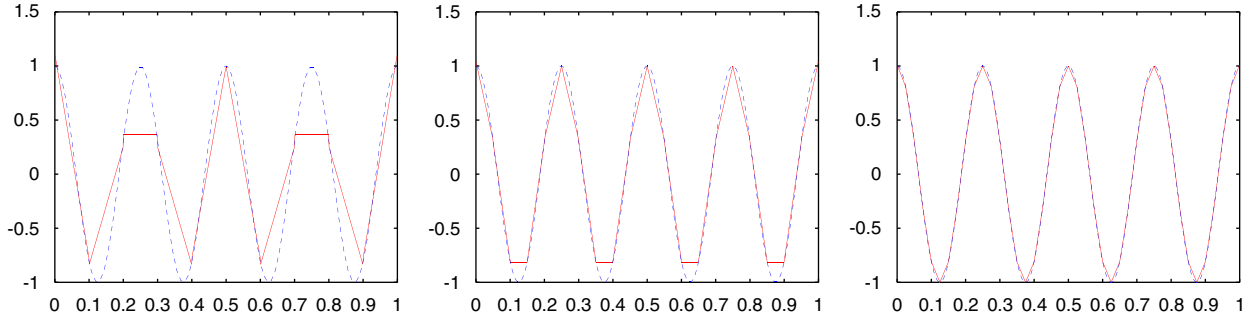

Fig. 4. $p = 1$, $\sigma = 4.5$: $\mathcal{N}_h = 10$ (left), $\mathcal{N}_h = 20$ (center), $\mathcal{N}_h = 40$ (right).

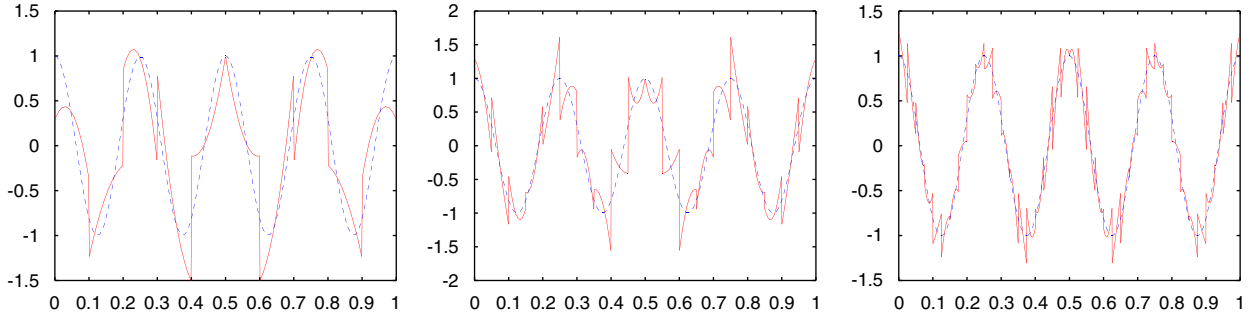

Fig. 5. $p = 2$, $\sigma = 1.375$: $\mathcal{N}_h = 10$ (left), $\mathcal{N}_h = 20$ (center), $\mathcal{N}_h = 40$ (right).

Please cite this article as: Y. Epshteyn, B. Rivière, Estimation of penalty parameters for symmetric interior penalty Galerkin methods, Journal of Computational and Applied Mathematics (2006), doi: 10.1016/j.cam.2006.08.029

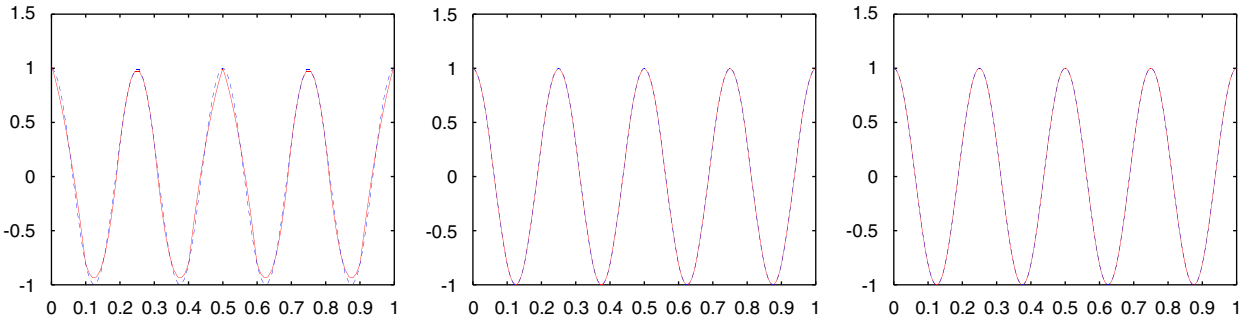

Fig. 6. $p = 2$, $\sigma = 12$: $\mathcal{N}_h = 10$ (left), $\mathcal{N}_h = 20$ (center), $\mathcal{N}_h = 40$ (right).

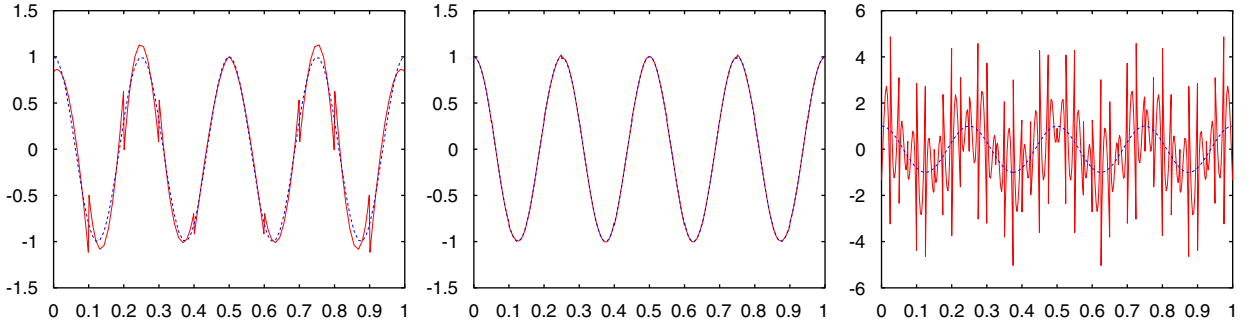

Fig. 7. $p = 3$, $\sigma = 3.5832$: $\mathcal{N}_h = 10$ (left), $\mathcal{N}_h = 20$ (center), $\mathcal{N}_h = 40$ (right).

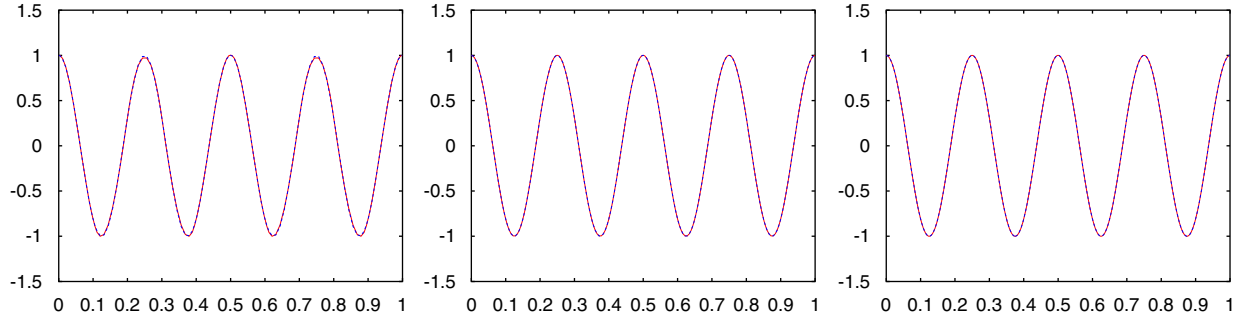

Fig. 8. $p = 3$, $\sigma = 23$: $\mathcal{N}_h = 10$ (left), $\mathcal{N}_h = 20$ (center), $\mathcal{N}_h = 40$ (right).

4.1. One-dimensional problem

We first consider the case of piecewise linears on several meshes containing 10, 20 and 40 intervals, respectively. In all figures, the exact solution is drawn as a dashed line whereas the numerical solution is drawn as a solid line. For a penalty value $\sigma = 0.5$ that is smaller than $\sigma^{**} = 2$, oscillations occur for all three meshes (see Fig. 3) and the numerical error is large. When $\sigma > \sigma^{**}$, the numerical solution is accurate (see Fig. 4). The two curves coincide with each other. The errors decrease as the mesh is refined according to the theoretical convergence rate given in Theorem 4.

We repeat the numerical experiments with piecewise quadratics and piecewise cubics. Unstable solutions are obtained for penalty values below the threshold value (see Figs. 5 and 7). The stable and convergent solutions are shown in Figs. 6–8. It is interesting to point that for the unstable penalty $\sigma = 3.5832$, the solution is accurate for the mesh with 20 elements; however large oscillations occur on meshes with 10 and 40 elements. Finally, Fig. 9 corresponds to a zero

Please cite this article as: Y. Epshteyn, B. Rivière, Estimation of penalty parameters for symmetric interior penalty Galerkin methods, Journal of Computational and Applied Mathematics (2006), doi: 10.1016/j.cam.2006.08.029

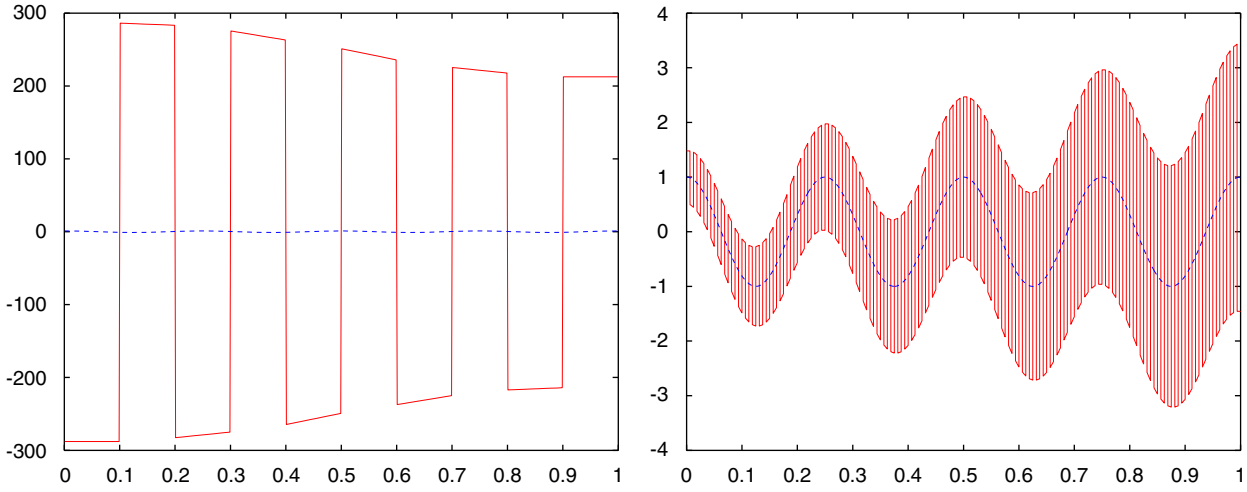

Fig. 9. $p = 1$, $\sigma = 0$: coarse mesh $\mathcal{N}_h = 10$ (left) and refined mesh $\mathcal{N}_h = 160$ (right).

Table 1
Numerical errors for one-dimensional simulations

$\mathcal{N}_h$	p	σ_n	$\sigma_n^{**-} = \sigma_n^{**+}$ $n = 0, N$	σ_n^{**} $0 < n < N$	L^2 error	H_0^1 error
10	1	0	1	2	251.7794	89.7737
160	1	0	1	2	1.5748	2.1370
10	1	0.5	1	2	1.4784	19.1598
10	1	4.5	1	2	0.2471	11.7768
20	1	0.5	1	2	1.1143	40.2011
20	1	4.5	1	2	0.0827	6.4208
40	1	0.5	1	2	0.1334	9.7604
40	1	4.5	1	2	0.0236	3.2528
10	2	1.375	4	8	0.3166	13.8863
10	2	12	4	8	0.0507	4.0257
20	2	1.375	4	8	0.2620	22.1197
20	2	12	4	8	0.0061	1.0534
40	2	1.375	4	8	0.1265	21.1470
40	2	12	4	8	7.3194×10^{-4}	0.2661
10	3	3.5832	9	18	0.1111	9.4328
10	3	23	9	18	0.0072	0.8487
20	3	3.5832	9	18	0.0072	1.2450
20	3	23	9	18	5.2545×10^{-4}	0.1124
40	3	3.5832	9	18	1.3497	467.8889
40	3	23	9	18	3.5184×10^{-5}	0.0141

penalty on a coarse mesh and a very fine mesh: as expected, refining the mesh is not enough to recover from the loss of coercivity.

A more precise estimate of the accuracy is given in Table 1. The absolute L^2 error $\|u - u_h\|_\Omega$ and H_0^1 error $(\sum_{E\in\mathcal{T}_h} \|\nabla(u - u_h)\|_E^2)^{1/2}$ are computed for each simulation. We also indicate the limiting penalty values given by (28). For stable solutions, we choose penalty values that are greater than the limiting value. It is to be noted that when σ is very close to the threshold penalty value, the coercivity constant C^* is very close to zero. In that case, numerical oscillations could still occur. This poor coercivity property is discussed in detail in [13].

Next, we numerically investigate the sharpness of the theoretical threshold values of the penalty parameter. On a fixed mesh containing thirty intervals, we increase the penalty parameter with a small enough step size (chosen here

Please cite this article as: Y. Epshteyn, B. Rivière, Estimation of penalty parameters for symmetric interior penalty Galerkin methods, Journal of Computational and Applied Mathematics (2006), doi: 10.1016/j.cam.2006.08.029

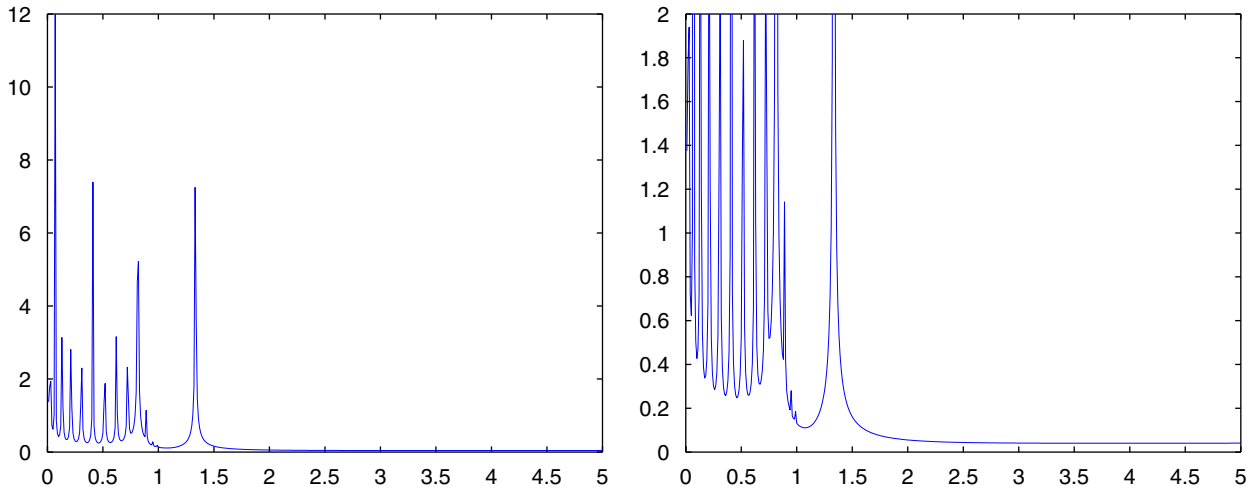

Fig. 10. Variation of L^2 error with respect to penalty parameter: mesh with 30 elements and piecewise linear approximation.

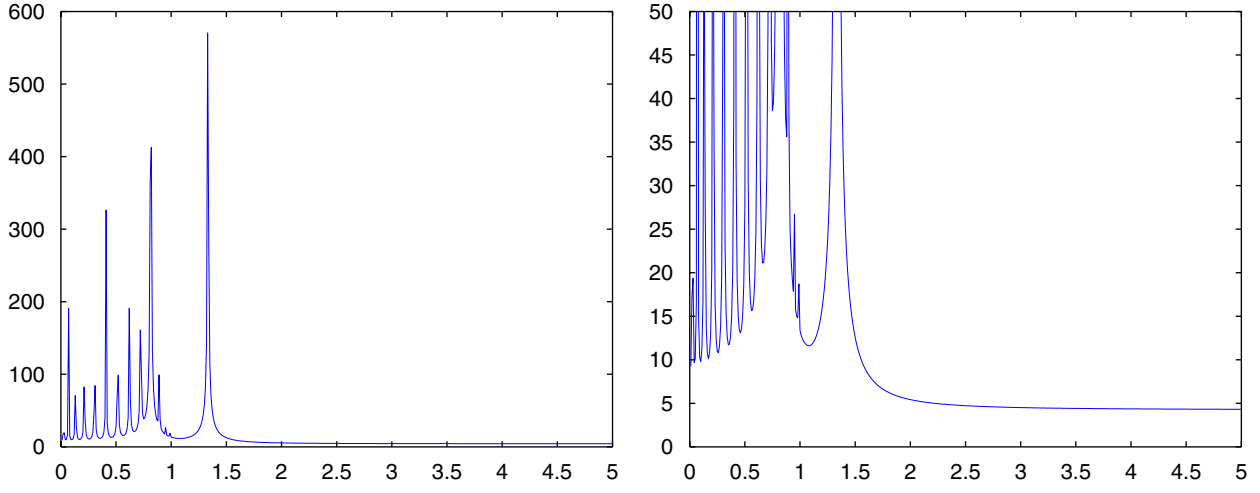

Fig. 11. Variation of H_0^1 error with respect to penalty parameter: mesh with 30 elements and piecewise linear approximation.

equal to 0.01) and we compute the absolute L^2 and H_0^1 norms of the error. The results are shown in Figs. 10–15, where the figures to the right are close-up views of the figures to the left. The polynomial degree is chosen to be equal to one, two or three everywhere. From these figures, we conclude that a stable numerical bound for the penalty parameter is 2 for piecewise linear approximation, 5 for piecewise quadratic approximation and 13 for piecewise cubic approximation. Those values are close to the theoretical bounds which are 2, 8 and 18, respectively. Theoretically, we proved that the threshold values are independent of the mesh size. We confirm this numerically by repeating the experiments on a more refined mesh (see Figs. 16 and 17). The same numerical bounds as for the coarser mesh are obtained.

4.2. Two-dimensional problem

4.2.1. Structured 2D mesh

We solve the problem on the structured mesh shown in Fig. 18. For this mesh, the smallest angle is $\theta_{\mathcal{T}} = \pi/4$. The exact solution for reference is shown in Fig. 19. In Fig. 20, we first consider polynomial degree equal to one on a very fine mesh (2048 elements). The penalty parameter is equal to either 0 or 3 everywhere. We also compute the solution

Please cite this article as: Y. Epshteyn, B. Rivière, Estimation of penalty parameters for symmetric interior penalty Galerkin methods, Journal of Computational and Applied Mathematics (2006), doi: 10.1016/j.cam.2006.08.029

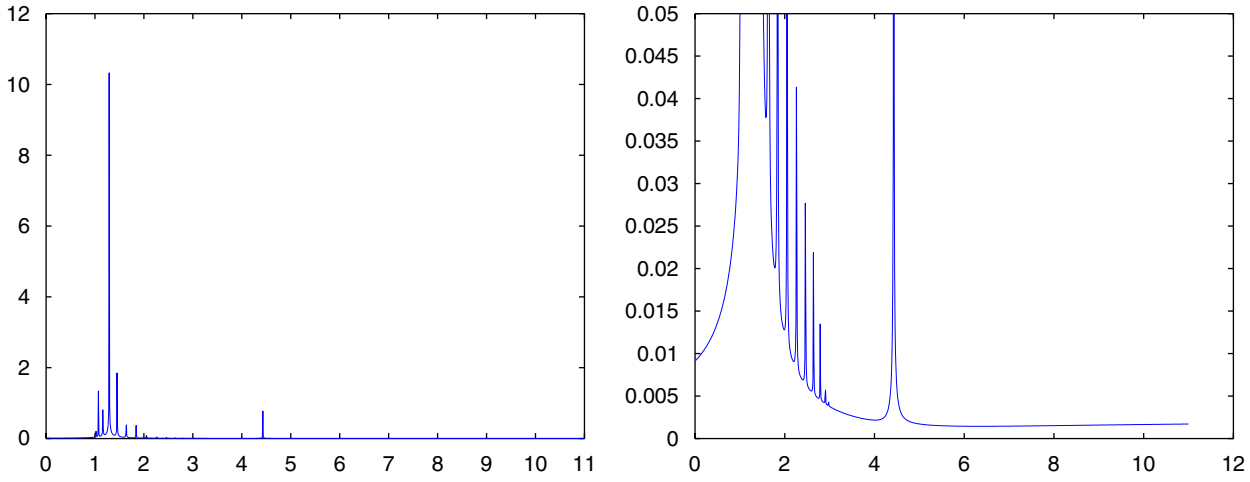

Fig. 12. Variation of L^2 error with respect to penalty parameter: mesh with 30 elements and piecewise quadratic approximation.

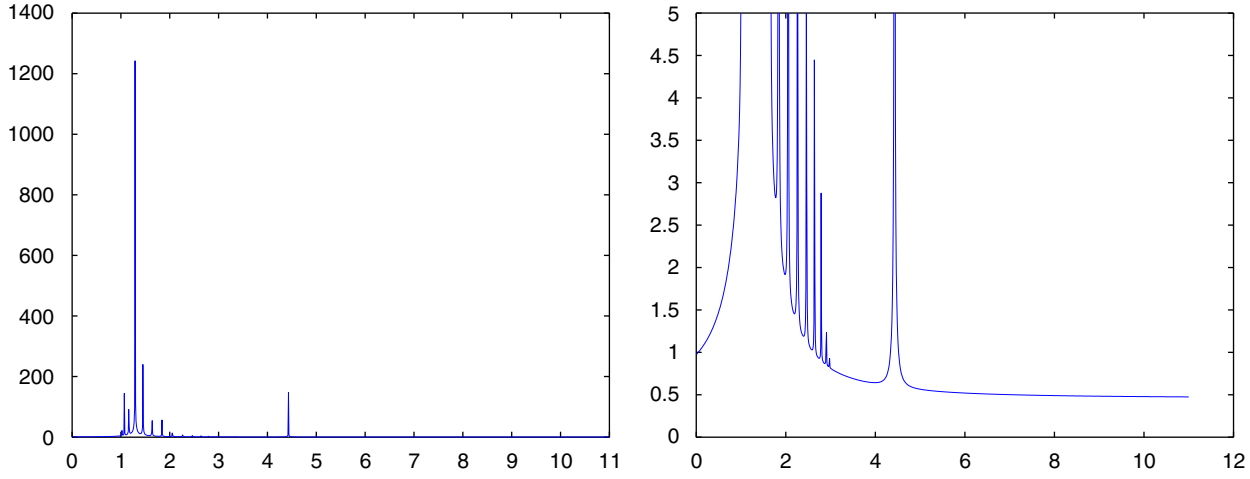

Fig. 13. Variation of H_0^1 error with respect to penalty parameter: mesh with 30 elements and piecewise quadratic approximation.

with a penalty parameter equal to $\sigma_I = 8$ on all interior edges and $\sigma_D = 14$ on all boundary edges. From (46)–(47), the threshold value is $\sigma_I^{**} = 6$ for the interior edges and $\sigma_D^{**} = 12$ for the boundary edges. For a penalty value above the limiting value, no oscillations occur whereas for a smaller penalty value, the solution is unstable. Fig. 21 shows the piecewise quadratic solution on a mesh containing 512 elements. Finally, for the case of piecewise cubic polynomials, the solutions are shown in Fig. 22 for a mesh containing 128 elements. We also present the solutions obtained by SIPG with a zero penalty. In this case, the standard proof for SIPG is not valid.

We give the error in the L^2 norm and the H_0^1 norm for all cases and we also give the limiting value $(\sigma_I^{**}, \sigma_D^{**})$ in Table 2. For a given penalty, the error decreases as the mesh is refined. Similar conclusions as in the one-dimensional case can be made. For stable methods, the error decreases with the right convergence rate. For unstable methods, oscillations may occur.

We present in Fig. 23 the numerical convergence of the SIPG solution for a "good" penalty value (larger than $\sigma_I^{**} = 6$ for the interior edges and $\sigma_D^{**} = 12$ for the boundary edges) and a "bad" penalty value (smaller than σ_I^{**}, σ_D^{**}). Piecewise linear approximation is used. The stable solution converges with the expected convergence rate ($\mathcal{O}(h^2)$ for the L^2 error and $\mathcal{O}(h)$ for the H^1 error) whereas the unstable solution does not converge as the mesh size decreases.

Please cite this article as: Y. Epshteyn, B. Rivière, Estimation of penalty parameters for symmetric interior penalty Galerkin methods, Journal of Computational and Applied Mathematics (2006), doi: 10.1016/j.cam.2006.08.029

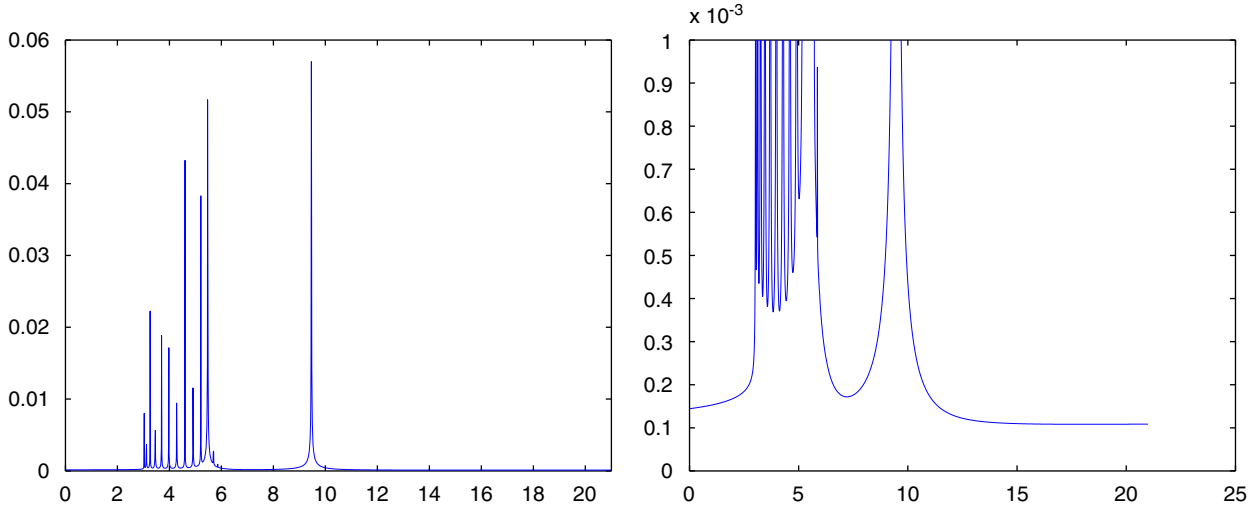

Fig. 14. Variation of L^2 error with respect to penalty parameter: mesh with 30 elements and piecewise cubic approximation.

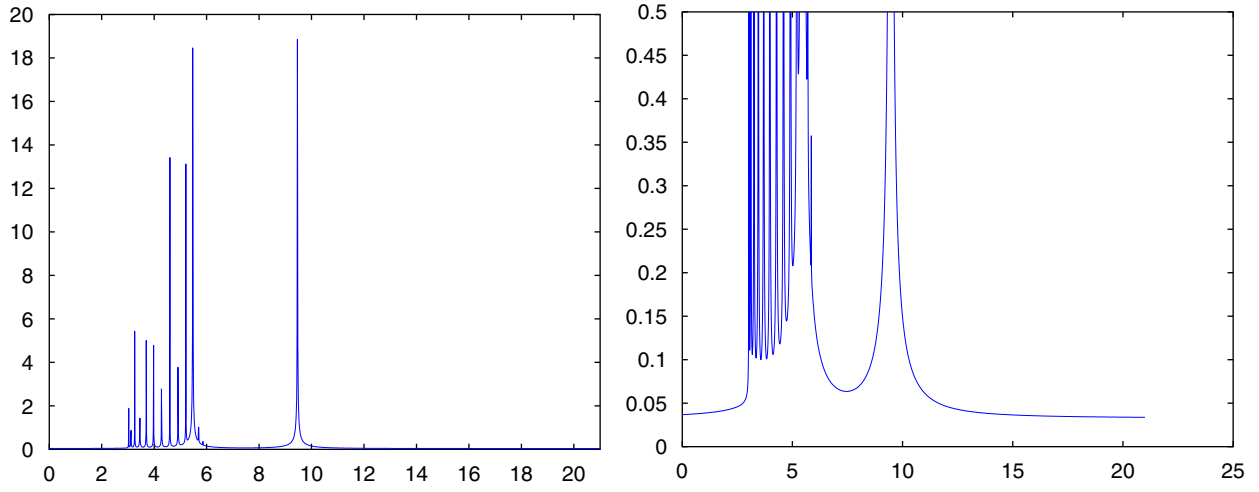

Fig. 15. Variation of H_0^1 error with respect to penalty parameter: mesh with 30 elements and piecewise cubic approximation.

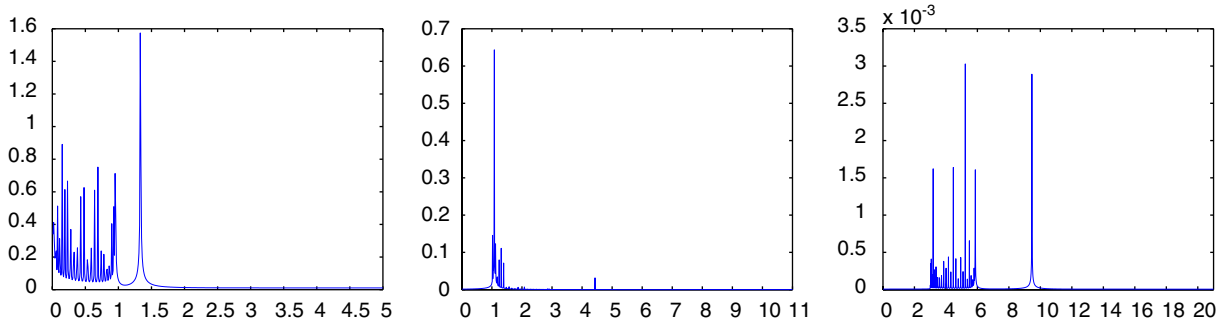

Fig. 16. Variation of L^2 error with respect to penalty parameter: mesh with 60 elements and polynomial approximation of degree one (left), two (center) and three (right).

Please cite this article as: Y. Epshteyn, B. Rivière, Estimation of penalty parameters for symmetric interior penalty Galerkin methods, Journal of Computational and Applied Mathematics (2006), doi: 10.1016/j.cam.2006.08.029

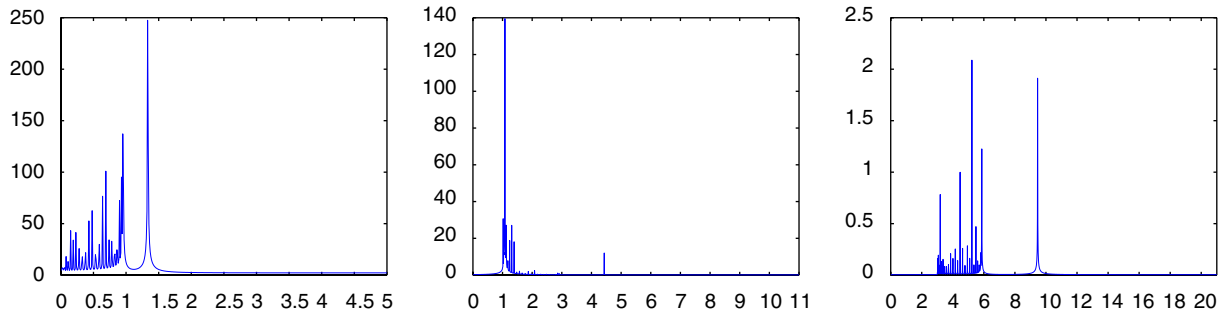

Fig. 17. Variation of H_0^1 error with respect to penalty parameter: mesh with 60 elements and polynomial approximation of degree one (left), two (center) and three (right).

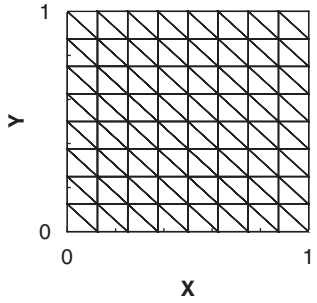

Fig. 18. Structured mesh with 128 elements.

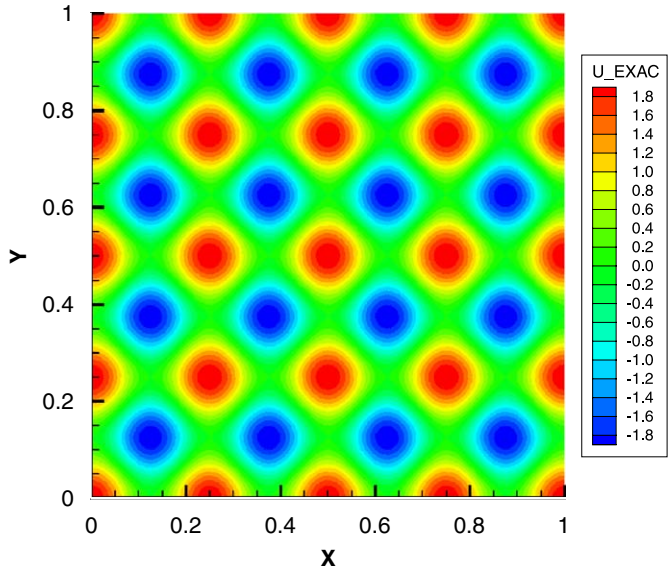

Fig. 19. Exact solution.

As in the 1D case, we numerically study the bound for the penalty values by computing the L^2 and H_0^1 errors for several penalty parameters on a mesh containing 128 elements. The penalty value for the boundary edges is taken equal to twice the penalty value for the interior edges. Figs. 24 and 25 show both errors for piecewise linear approximation

Please cite this article as: Y. Epshteyn, B. Rivière, Estimation of penalty parameters for symmetric interior penalty Galerkin methods, Journal of Computational and Applied Mathematics (2006), doi: 10.1016/j.cam.2006.08.029

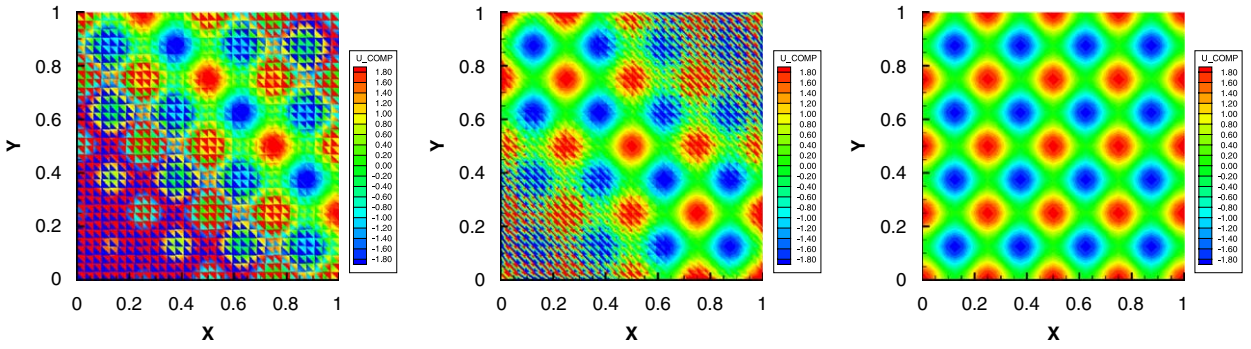

Fig. 20. Computed solution for piecewise linear approximation and $\mathcal{N}_h = 2048$ elements: $\sigma = 0$ (left), $\sigma = 3$ (center), $\sigma_I = 8$, $\sigma_D = 14$ (right).

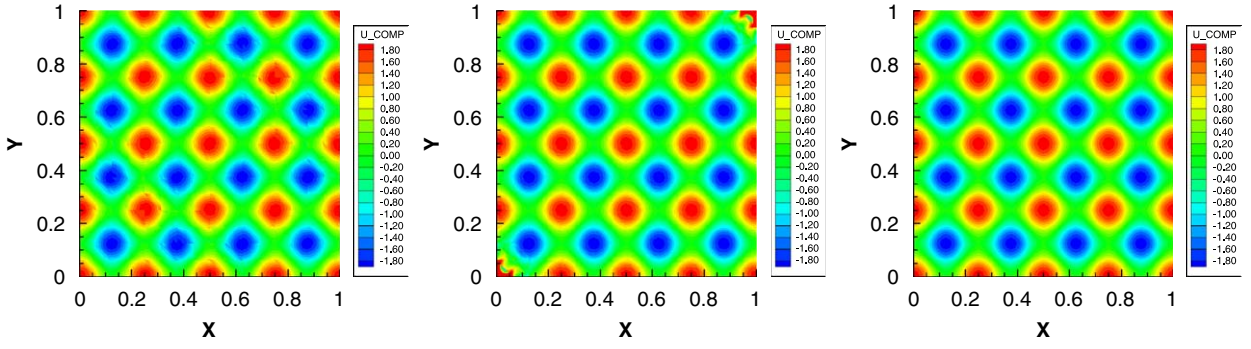

Fig. 21. Numerical solution for piecewise quadratic approximation and $\mathcal{N}_h = 512$ elements: $\sigma = 0$ (left), $\sigma = 4.5$ (center), $\sigma_I = 20$, $\sigma_D = 38$ (right).

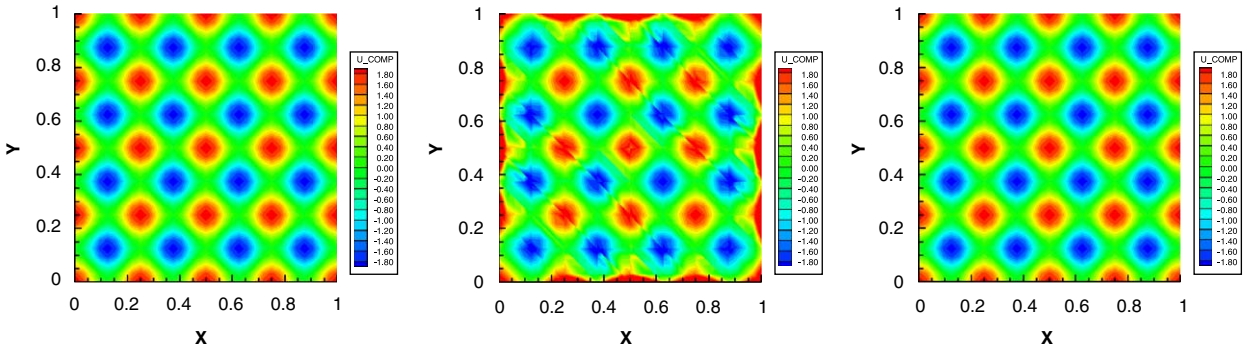

Fig. 22. Numerical solution for piecewise cubic approximation and $\mathcal{N}_h = 128$ elements: $\sigma = 0$ (left), $\sigma = 11$ (center), $\sigma_I = 38$, $\sigma_D = 74$ (right).

whereas Figs. 26 and 27 show the errors for piecewise quadratic approximation. The numerical bounds for the interior penalty values are equal to 4 for $p = 1$ and 10 for $p = 2$ whereas the theoretical bounds for the interior penalty values are 6 and 18, respectively.

4.2.2. Unstructured 2D mesh

We consider an unstructured triangular mesh containing 219 elements (see Fig. 28). We present the results for the case of piecewise quadratic approximations. As before we vary the penalty parameters $\sigma = 0, 7.5$ for the choice of bad penalty and we pick good penalty at each edge separately using theoretical values for the threshold penalty. Here, the value of $\cot\theta$ varies between 0.5821 and 2.1578 and thus, the limiting penalty parameter takes different values for each edge. The numerical solutions are shown in Fig. 29.

Please cite this article as: Y. Epshteyn, B. Rivière, Estimation of penalty parameters for symmetric interior penalty Galerkin methods, Journal of Computational and Applied Mathematics (2006), doi: 10.1016/j.cam.2006.08.029

Table 2
Numerical errors for two-dimensional simulations

$\mathcal{N}_h$	p	σ_I	σ_D	σ_I^{**}	σ_D^{**}	L^2 error	H_0^1 error
2048	1	0	0	6	12	1.6208681	7.9950783
2048	1	3	3	6	12	9.7490787×10^{-1}	1.8162526×10^{2}
2048	1	8	14	6	12	4.0349201×10^{-2}	5.1780241
512	2	0	0	18	36	5.2324755×10^{-2}	4.3847913
512	2	4.5	4.5	18	36	1.7144388×10^{-1}	20.100636
512	2	20	38	18	36	1.3266233×10^{-2}	2.0443066
128	3	0	0	36	72	7.8099710×10^{-3}	6.0682964×10^{-1}
128	3	11	11	36	72	2.1133410×10^{-1}	25.599158
128	3	38	74	36	72	6.0859298×10^{-3}	4.7570410×10^{-1}

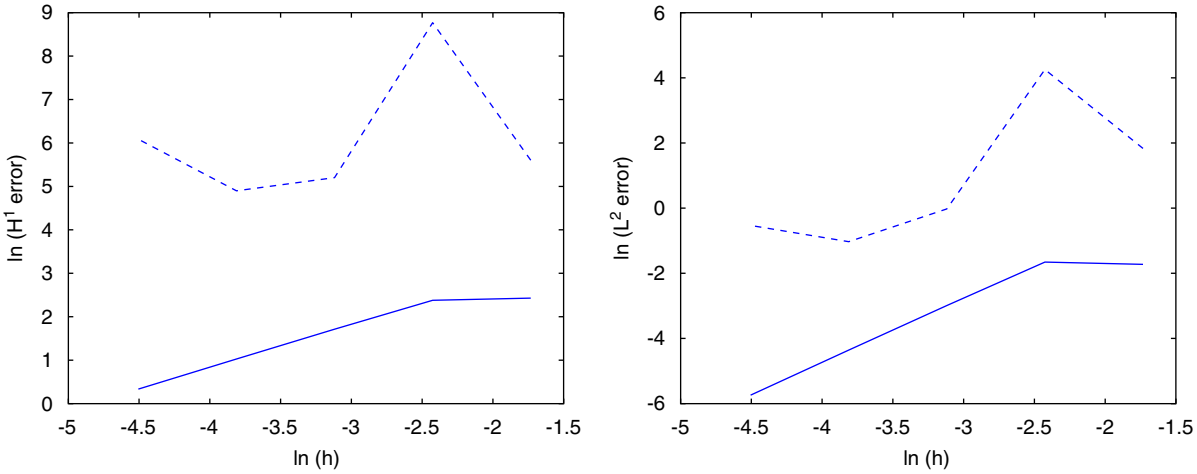

Fig. 23. Numerical convergence rates for the case $\sigma = 3$ (dashed line) and $\sigma_I = 8$, $\sigma_D = 14$ (solid line): H_0^1 errors (left) and L^2 errors (right). The threshold penalty values are $\sigma_I^{**} = 6$, $\sigma_D^{**} = 12$.

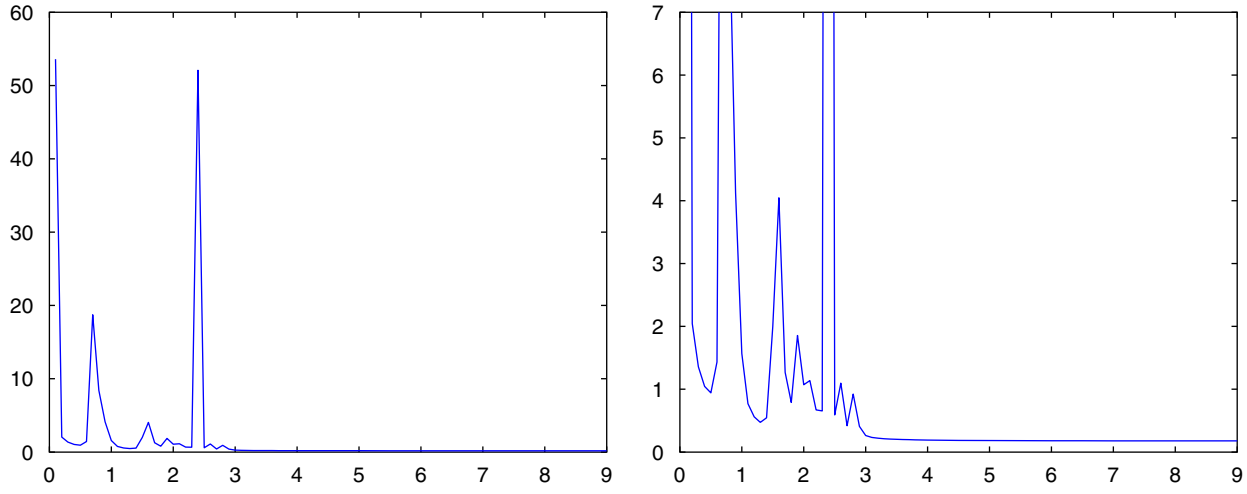

Fig. 24. Variation of L^2 error with respect to penalty parameter for the structured mesh with 128 elements and piecewise linear approximation.

Please cite this article as: Y. Epshteyn, B. Rivière, Estimation of penalty parameters for symmetric interior penalty Galerkin methods, Journal of Computational and Applied Mathematics (2006), doi: 10.1016/j.cam.2006.08.029

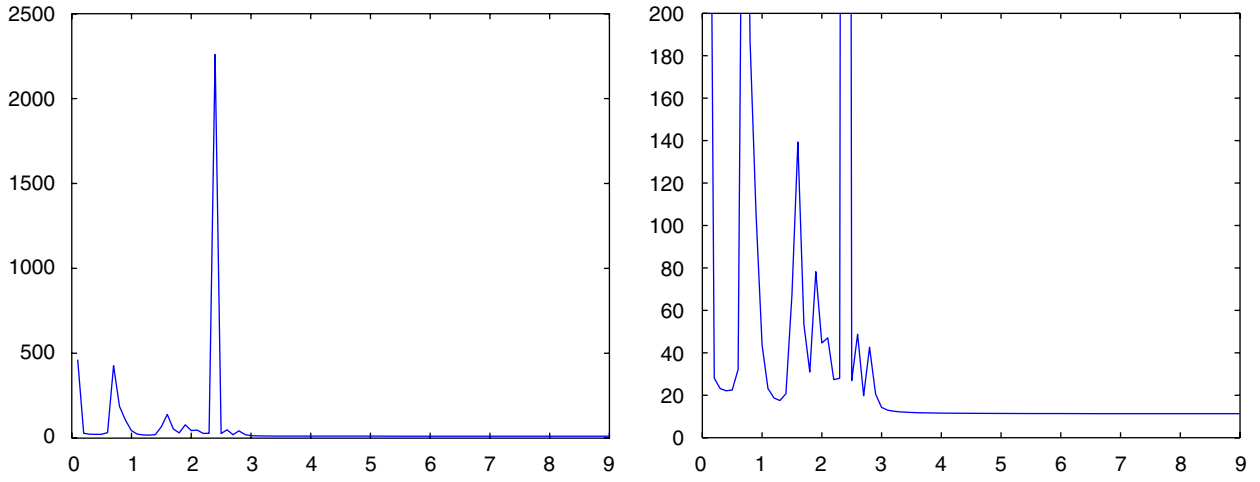

Fig. 25. Variation of H_0^1 error with respect to penalty parameter for the structured mesh with 128 elements and piecewise linear approximation.

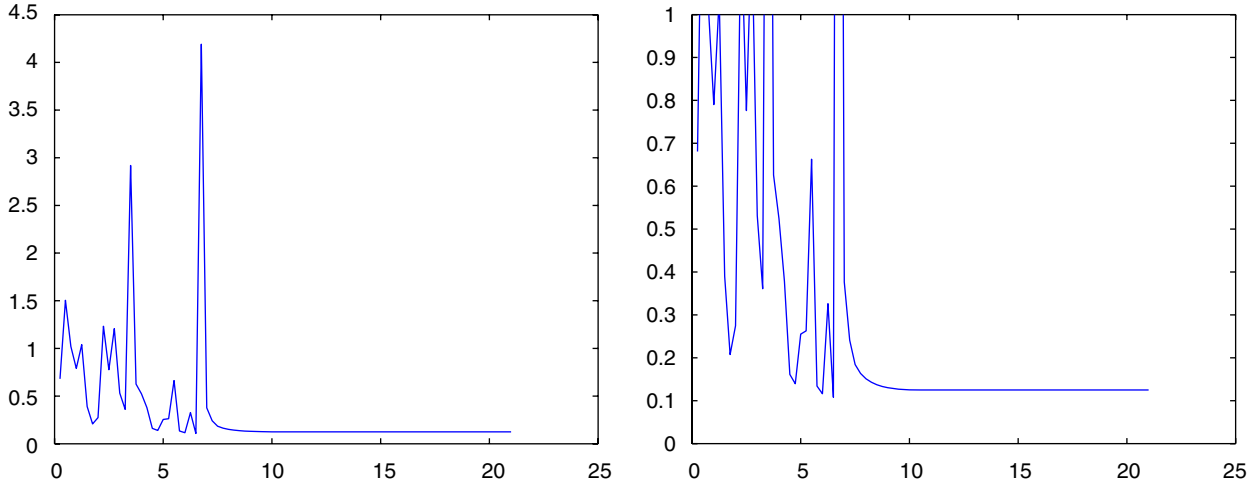

Fig. 26. Variation of L^2 error with respect to penalty parameter for the structured mesh with 128 elements and piecewise quadratic approximation.

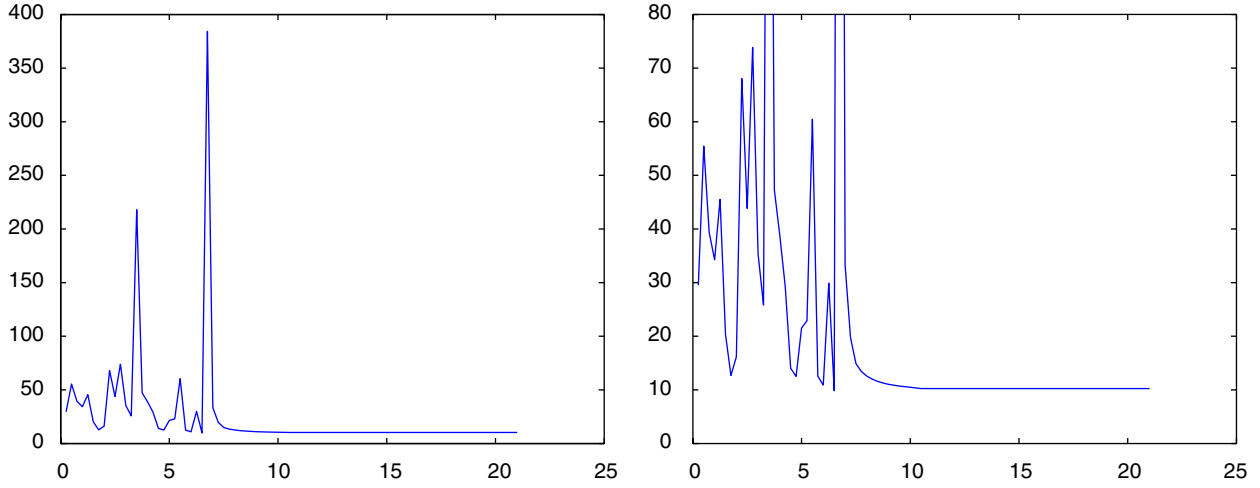

Fig. 27. Variation of H_0^1 error with respect to penalty parameter for the structured mesh with 128 elements and piecewise quadratic approximation.

Please cite this article as: Y. Epshteyn, B. Rivière, Estimation of penalty parameters for symmetric interior penalty Galerkin methods, Journal of Computational and Applied Mathematics (2006), doi: 10.1016/j.cam.2006.08.029

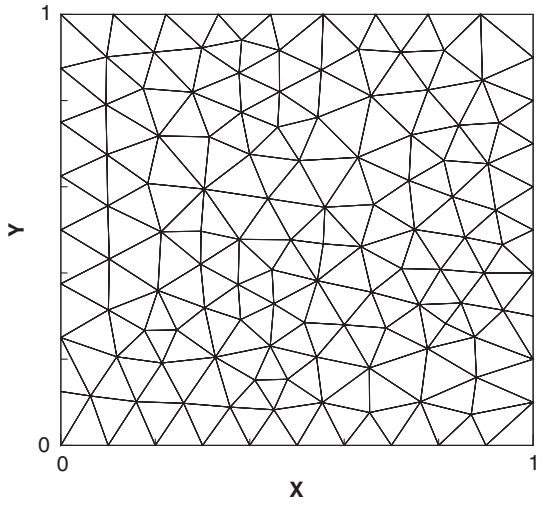

Fig. 28. Unstructured mesh with 219 elements.

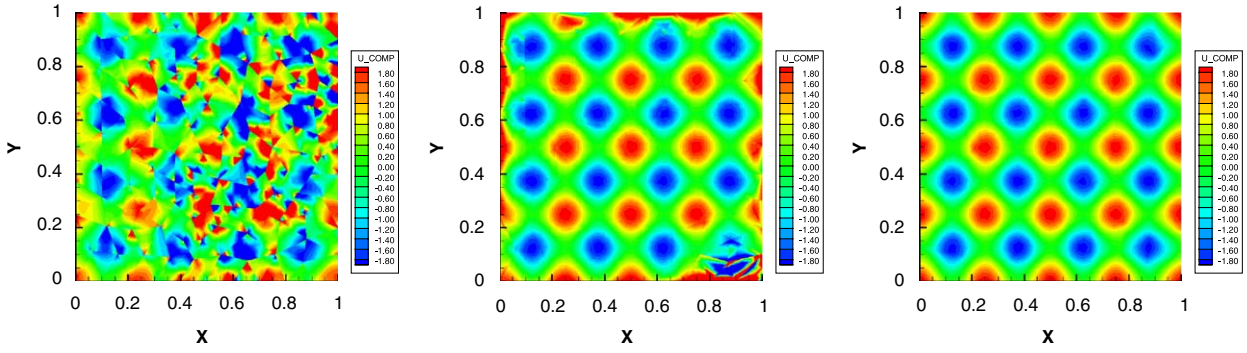

Fig. 29. Numerical solution on unstructured mesh for piecewise quadratic solution: $\sigma = 0$ (left), $\sigma = 7.5$ (center), good $\sigma = \sigma_e$ (right).

Table 3
Numerical errors for two-dimensional unstructured mesh simulations

$\mathcal{N}_h$	p	σ_e	L^2 error	H_0^1 error
219	2	0	1.0262113	52.510991
219	2	7.5	6.3221136×10^{-1}	66.159341
219	2	σ_e	4.3241933×10^{-2}	4.7130677
876	2	0	5.5677943×10^{-2}	5.8047835
876	2	7.5	2.2284393×10^{-2}	4.3895847
876	2	σ_e	5.2956025×10^{-3}	1.2169522

We present the numerical errors in the L^2 and H_0^1 norms in Table 3. Those errors are computed on the initial mesh and a uniformly refined mesh containing 876 elements.

Figs. 30 and 31 show the effects of the penalty value on the L^2 and H_0^1 errors and give a numerical bound for the penalty equal to 14. We perform several simulations such that the penalty values increases uniformly from 0.01 to 21 and such that for each simulation the penalty parameter is constant over all edges. From (46), (47), the theoretical threshold penalty values vary from edge to edge, with an average equal to 17.4403.

Please cite this article as: Y. Epshteyn, B. Rivière, Estimation of penalty parameters for symmetric interior penalty Galerkin methods, Journal of Computational and Applied Mathematics (2006), doi: 10.1016/j.cam.2006.08.029

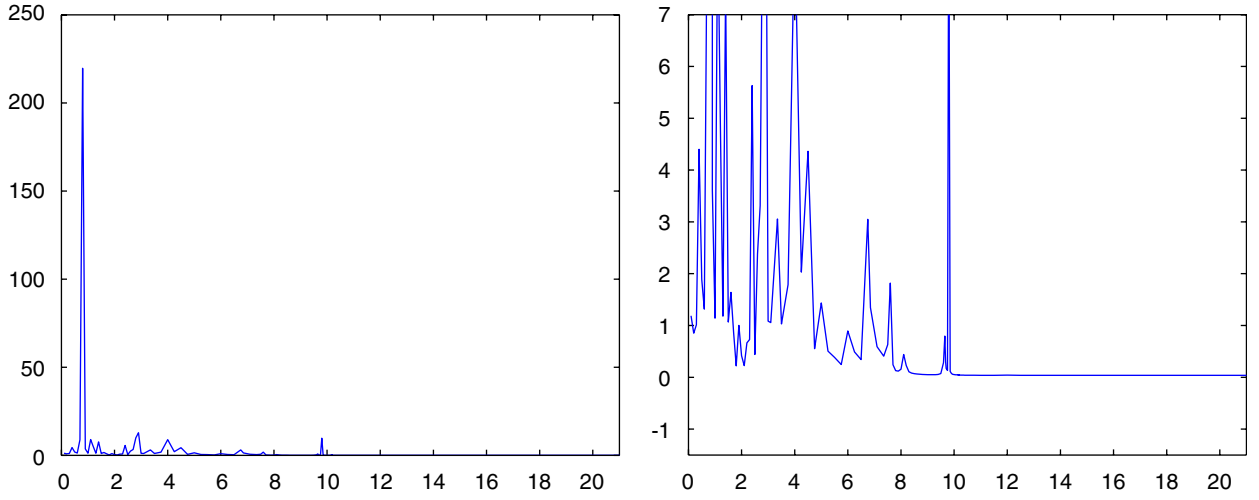

Fig. 30. Variation of L^2 error with respect to penalty values for piecewise quadratic approximation.

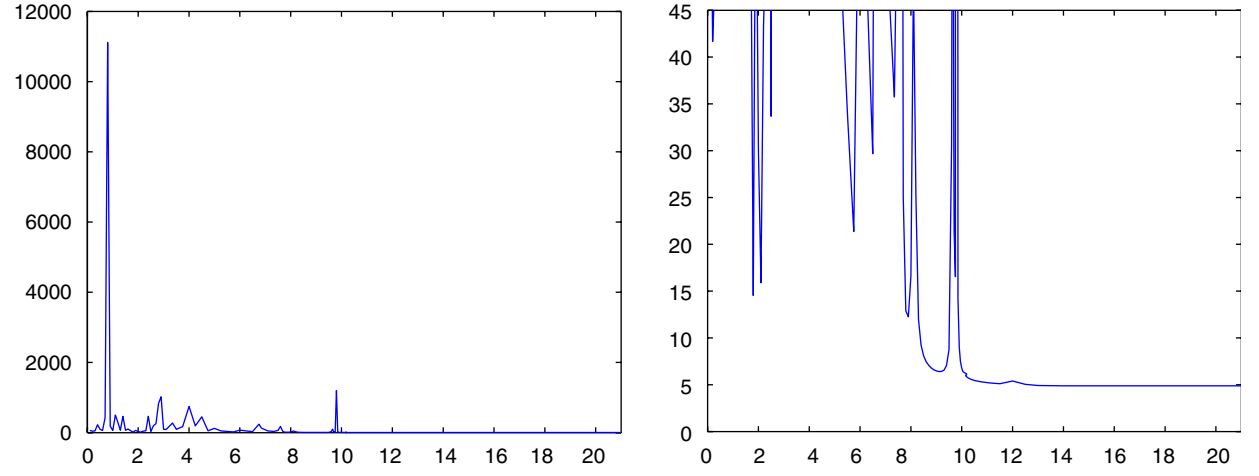

Fig. 31. Variation of H_0^1 error with respect to penalty values for piecewise quadratic approximation.

4.2.3. 2D mesh with localized poor elements

In this example, we numerically investigate the influence of a local mesh singularity due to a "flat" triangle. The mesh is given in Fig. 32. It consists of regular triangles with $\cot\theta_E = 1$ except in a small region where $\cot\theta_E$ takes the values $\{1.75, 2, 3.667\}$. In this experiment, we choose the penalty parameter σ constant on all interior edges except the edges denoted $e_1, \ldots, e_6$ (see Fig. 32). From Eqs. (46), (47), we choose $\sigma_{e_1} = 1.5\sigma$, $\sigma_{e_2} = 1.375\sigma$, $\sigma_{e_3} = 1.875\sigma$, $\sigma_{e_4} = 2.8333\sigma$, $\sigma_{e_5} = 2.7083\sigma$ and $\sigma_{e_6} = 2.3333\sigma$. The penalty value for the boundary edges is taken equal to 2σ. We then vary σ in the interval $[0, 21]$ and compute the L^2 and H_0^1 errors. From Figs. 33 and 34, we obtain the numerical bound $\sigma = 13$, which is close to the theoretical value equal to 18. For a penalty greater than 13, the L^2 error is constant equal to 0.250. In a second experiment, we fix the penalty value to 13 everywhere and the resulting L^2 error increases to 0.856. Clearly, this shows the effect of a few "bad" mesh elements on the overall stability and accuracy of the solution.

Please cite this article as: Y. Epshteyn, B. Rivière, Estimation of penalty parameters for symmetric interior penalty Galerkin methods, Journal of Computational and Applied Mathematics (2006), doi: 10.1016/j.cam.2006.08.029

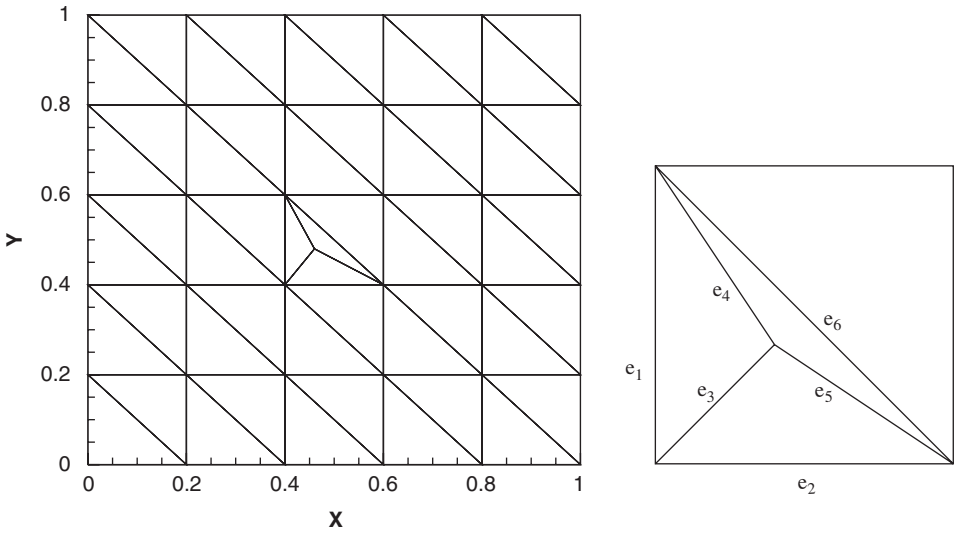

Fig. 32. 2D mesh with localized poor elements (left) with close-up view (right).

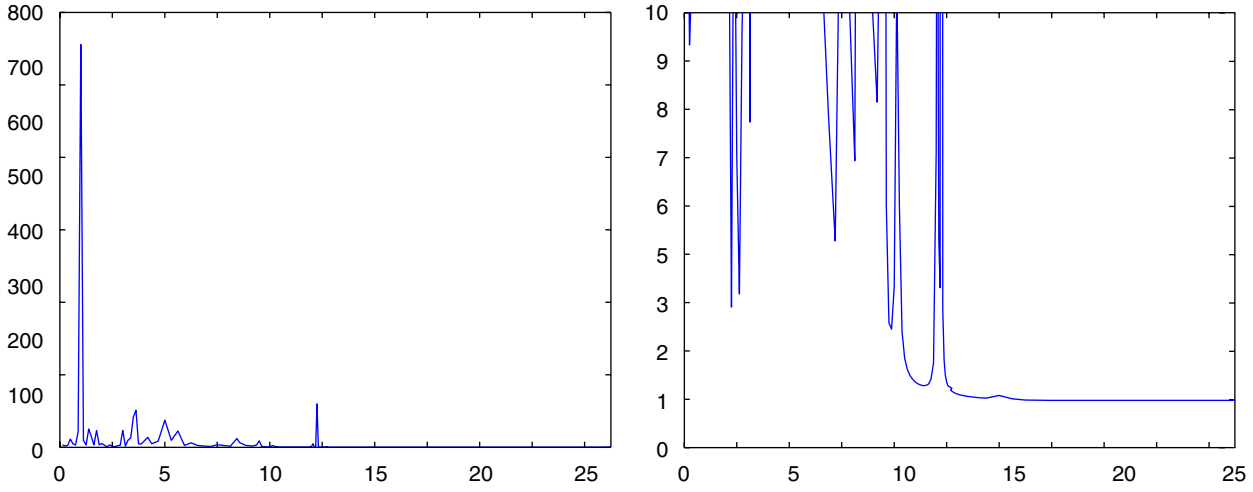

Fig. 33. Variation of L^2 error with respect to penalty parameter for piecewise quadratic approximation.

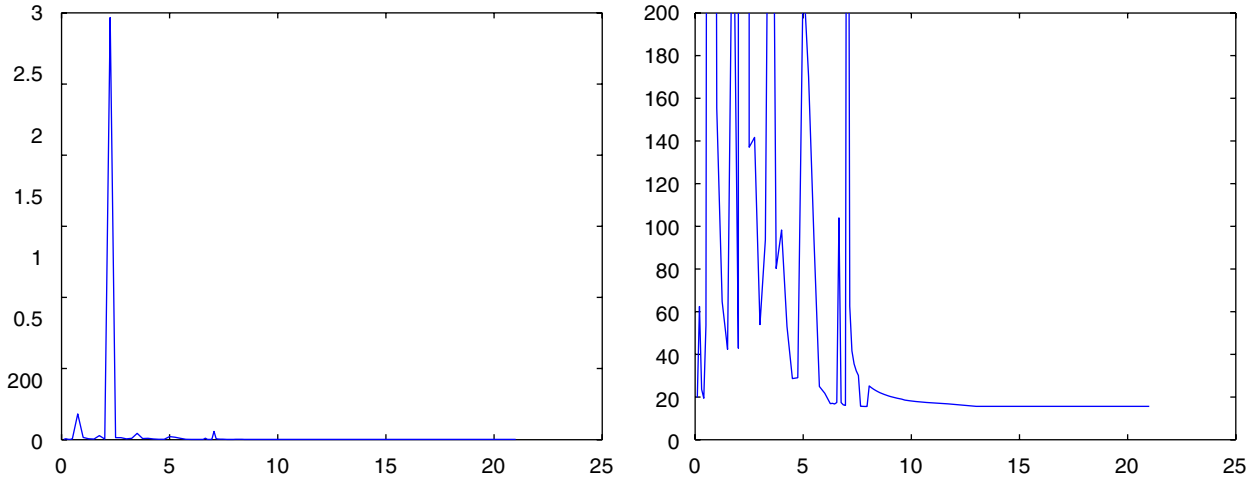

Fig. 34. Variation of H_0^1 error with respect to penalty parameter for piecewise quadratic approximation.

Please cite this article as: Y. Epshteyn, B. Rivière, Estimation of penalty parameters for symmetric interior penalty Galerkin methods, Journal of Computational and Applied Mathematics (2006), doi: 10.1016/j.cam.2006.08.029

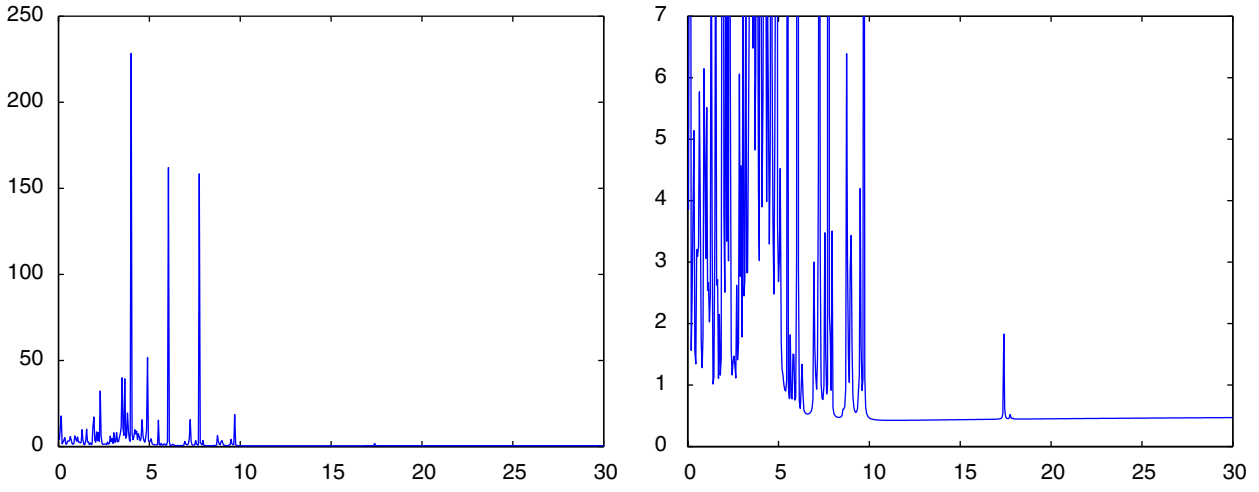

Fig. 35. Variation of L^2 error with respect to the penalty value for piecewise quadratic approximation.

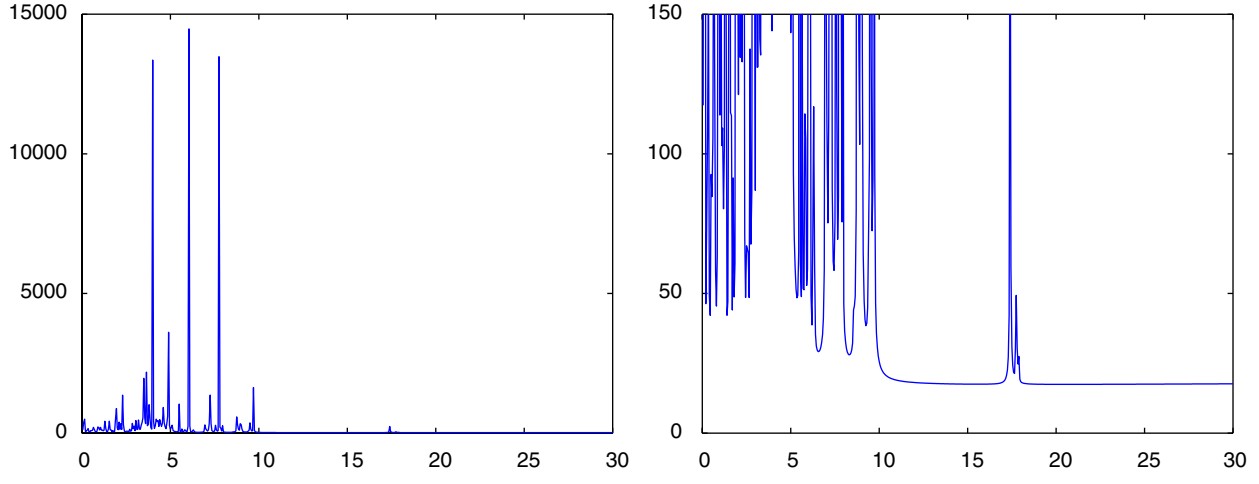

Fig. 36. Variation of H_0^1 error with respect to the penalty value for piecewise quadratic approximation.

4.3. Three-dimensional problem

We first explain how to obtain the angle $\theta_{\mathscr{T}}$. The value $|\cot\ \theta_{\mathscr{T}}|$ is the maximum of $|\cot\ \theta_E|$ over all mesh elements E. For a given element E, the angle θ_E is the one that yields the smallest $\sin\theta_{E,\xi}$ over all edges ξ of the tetrahedron. We now explain how to obtain $\theta_{E,\xi}$ for given E and ξ.

(1) Compute the equations of the planes corresponding to the two faces of E that share the common edge ξ.

$$i = 1, 2, \quad a^i_{E,\xi}x + b^i_{E,\xi}y + c^i_{E,\xi}z + d^i_{E,\xi} = 0.$$

(2) The normal vectors to those two faces are

$$i = 1, 2, \quad \mathbf{n}_{e_i} = (a^i_{E,\xi}, b^i_{E,\xi}, c^i_{E,\xi}).$$

(3) Compute $\cos\theta_{E,\xi}$ and $\sin\theta_{E,\xi}$:

$$\cos\theta_{E,\xi} = \mathbf{n}_{e_1} \cdot \mathbf{n}_{e_2}, \quad \sin\theta_{E,\xi} = (1 - (\cos\theta_{E,\xi})^2)^{1/2}.$$

Please cite this article as: Y. Epshteyn, B. Rivière, Estimation of penalty parameters for symmetric interior penalty Galerkin methods, Journal of Computational and Applied Mathematics (2006), doi: 10.1016/j.cam.2006.08.029

We now solve the problem on a mesh containing 720 tetrahedral elements such that $h \cot \mathscr{T}_h = 1$. We fix $\beta_0 = \frac{1}{2}$. Piecewise quadratic approximation is used. In Figs. 35 and 36, we plot the numerical L^2 and H_0^1 errors versus the penalty parameter chosen constant over all edges. The numerical bounds for the penalty value is equal to 18, which is close to the theoretical value 24 from (66).

5. Conclusions

By presenting lower bounds of the penalty parameter useful for practical computations, this paper removes one known disadvantage of the symmetric interior penalty methods, namely the fact that stability of the method is obtained for an unknown large enough penalty value. Even though we focused on the elliptic problems, our improved coercivity and continuity results can be applied to the analysis of the SIPG method for time-dependent problems.

References

[1] D.N. Arnold, An interior penalty finite element method with discontinuous elements, Ph.D. Thesis, The University of Chicago, 1979.
[2] D.N. Arnold, An interior penalty finite element method with discontinuous elements, SIAM J. Numer. Anal. 19 (1982) 742–760.
[3] D.N. Arnold, F. Brezzi, B. Cockburn, L.D. Marini, Unified analysis of discontinuous Galerkin methods for elliptic problems, SIAM J. Numer. Anal. 39 (5) (2002) 1749–1779.
[4] I. Babuška, The finite element method with penalty, Math. Comput. 27 (1973) 221–228.
[5] I. Babuška, M. Zlamal, Nonconforming elements in the finite element method with penalty, SIAM J. Numer. Anal. 10 (1973) 863–875.
[6] G.A. Baker, Finite element methods for elliptic equations using nonconforming elements, Math. Comput. 31 (137) (1977) 45–59.
[7] G.A. Baker, W.N. Jureidini, O.A. Karakashian, Piecewise solenoidal vector fields and the Stokes problem, SIAM J. Numer. Anal. 27 (1990) 1466–1485.
[8] R. Becker, P. Hansbo, R. Stenberg, A finite element method for domain decomposition with non-matching grids, M2AN Math. Model. Numer. Anal. 37 (2003) 209–225.
[9] P. Ciarlet, The Finite Element Method for Elliptic Problems, North-Holland, Amsterdam, 1978.
[10] B. Cockburn, G.E. Karniadakis, C.-W. Shu (Eds.), First International Symposium on Discontinuous Galerkin Methods, Lecture Notes in Computational Science and Engineering, vol. 11, Springer, Berlin, 2000.
[11] C. Dawson, S. Sun, M.F. Wheeler, Compatible algorithms for coupled flow and transport, Comput. Meth. Appl. Mech. Eng. 193 (2004) 2565–2580.
[12] J. Douglas, T. Dupont, Interior penalty procedures for elliptic and parabolic Galerkin methods, Lecture Notes in Physics, vol. 58, Springer, Berlin, 1976.
[13] A. Ern, J.-L. Guermond, Theory and practice of finite elements, Applied Mathematical Sciences, vol. 159, Springer, Berlin, 2003.
[14] V. Girault, B. Rivière, M.F. Wheeler, A discontinuous Galerkin method with non-overlapping domain decomposition for the Stokes and Navier–Stokes problems, Math. Comput. 74 (2005) 53–84.
[15] P. Houston, C. Schwab, E. Süli, Discontinuous hp-finite element methods for advection–diffusion reaction problems, SIAM J. Numer. Anal. 39 (6) (2002) 2133–2163.
[16] O.A. Karakashian, W. Jureidini, A nonconforming finite element method for the stationary Navier–Stokes equations, SIAM J. Numer. Anal. 35 (1998) 93–120.
[17] S. Kaya, B. Rivière, A discontinuous subgrid eddy viscosity method for the time-dependent Navier–Stokes equations, SIAM J. Numer. Anal. 43 (4) (2005) 1572–1595.
[18] J.R. Lee, The law of cosines in a tetrahedron, J. Korea Soc. Math. Ed. Ser. B: Pure Appl. Math. 4 (1997) 1–6.
[19] J.A. Nitsche, Uber ein Variationsprinzip zur Losung von Dirichlet-Problemen bei Verwendung von Teilraumen, die keinen Randbedingungen unteworfen sind, Abh. Math. Sem. Univ. Hamburg 36 (1971) 9–15.
[20] B. Rivière, V. Girault, Discontinuous finite element methods for incompressible flows on subdomains with non-matching interfaces, Comput. Meth. Appl. Mech. Eng. 195 (2006) 3274–3292.
[21] B. Rivière, M.F. Wheeler, V. Girault, A priori error estimates for finite element methods based on discontinuous approximation spaces for elliptic problems, SIAM J. Numer. Anal. 39 (3) (2001) 902–931.
[22] B. Rivière, I. Yotov, Locally conservative coupling of Stokes and Darcy flow, SIAM J. Numer. Anal. 42 (5) (2005) 1959–1977.
[23] S. Sun, M.F. Wheeler, Symmetric and nonsymmetric discontinuous Galerkin methods for reactive transport in porous media, SIAM J. Numer. Anal. 43 (1) (2005) 195–219.
[24] T. Warburton, J.S. Hesthaven, On the constants in hp-finite element trace inverse inequalities, Comput. Meth. Appl. Mech. Eng. 192 (2003) 2765–2773.
[25] M.F. Wheeler, An elliptic collocation-finite element method with interior penalties, SIAM J. Numer. Anal. 15 (1) (1978) 152–161.

Please cite this article as: Y. Epshteyn, B. Rivière, Estimation of penalty parameters for symmetric interior penalty Galerkin methods, Journal of Computational and Applied Mathematics (2006), doi: 10.1016/j.cam.2006.08.029